Accelerator Magnet System

Friday, 29 July, 2010 in Beijing , 16:15– 18:15

Ching-Shiang Hwang (黃清鄉)

(cshwang@srrc.gov.tw)

National Synchrotron Radiation Research Center (NSRRC), Hsinchu

Outlines

- Introduction to lattice magnets
- The magnet features of various accelerator magnets
- Magnet code for field calculation
- Field error source of magnet
- Magnetic field analysis of lattice magnet
- Introduction of pulse magnet
- Introduction of magnet field measurement

Introduction

1. Basic theorem for accelerator magnet type of electromagnets in the synchrotron radiation source.
2. The main properties and roles of accelerator magnets.
3. Magnet design should consider both in terms of physics of the components and the engineering constraints in practical circumstances.
4. The use of code for predicting flux density distributions and the iterative techniques used for pole face and coil design.
5. What parameters for accelerator magnet are required to design the magnet?
6. An example of NSRRC magnet system will be described and discussed.

Introduction of magnet arrangement

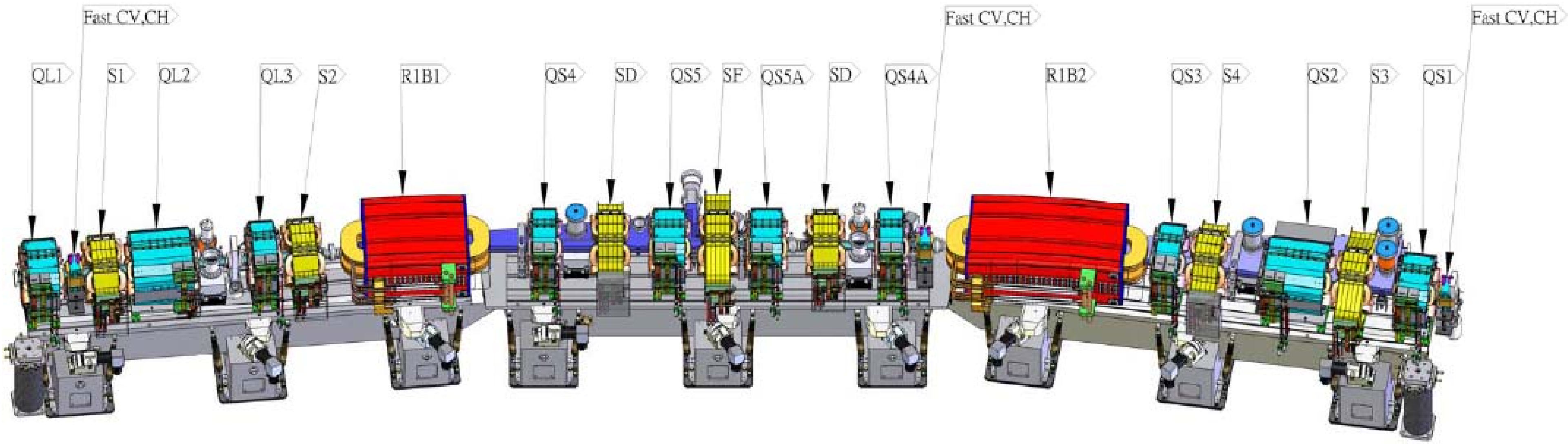

The magnet features of various accelerator magnets-1

◆Lorentz fource

$$\vec{F} = q(\vec{E} + \vec{v} \times \vec{B})$$

Although, the electric field appears in the Lorentz forces, but a magnetic field of one Tesla gives the same bending force as an electric field of 300 million Volts per meter for relativistic particles with velocity $v \approx c$.

∗ Magnets in storage ring

Dipole	-	bending and radiation
Quadrupole	-	focusing or defocusing
Sextupole	-	chromaticity correction
Corrector	-	small angle correction

The magnet features of various accelerator magnet-2

- **Magnetic field features of lattice magnets**

$$\Phi(x,y,z)=\sum_{m=0}^{\infty}\frac{(B_m(z)+i\,A_m(z))(x+iy)^{m+1}}{(m+1)}$$

Two sets of orthogonal multipoles with amplitude constants *Bm* and *Am* which represent the Normal and Skew multipoles components. The fields strength can be derived as

$$\vec{B}(x,y,z)=-\vec{\nabla}\Phi(x,y,z)$$

Therefore, the general magnetic field equation including only the most commonly used upright multipole components is given by

$$B_x = A_1\cdot x + A_2\cdot(x^2-y^2)+\frac{A_3}{6}\cdot(-3y^2x+x^3)+\ldots.$$

$$B_y = B_o + B_1\cdot x+\frac{B_2}{2}\cdot(x^2-y^2)+\frac{B_3}{6}\cdot(x^3-3xy^2)+\ldots.$$

where B_0,$B_1(A_1)$, $B_2(A_2)$,and $B_3(A_3)$ denote the harmonic field strength components and call it the normal (skew) dipole,quadrupole,sextupole and so on.

The magnet features of various accelerator magnet-2

- **Magnetic spherical harmonics derived from Maxwell's equations.**

Maxwell's equations for magneto-statics: $\vec{\nabla} \cdot \vec{B} = 0$, $\vec{\nabla} \times \vec{H} = \vec{j}$

No current excitation: $j = 0$

Then we can use : $\vec{B} = -\vec{\nabla}\Phi_M$

Therefore the Laplace's equation can be obtained as: $\nabla^2\Phi = 0$

where Φ_M is the magnetic scalar potential.

Thinking the two dimensional case (constant in the z direction) and solving for cylindrical coordinates (r,θ):

$$\Phi_M = (E + F\theta)(G + H \ln r)\sum_{n=1}^{\infty}\left(a_n r^n \cos n\theta + b_n r^n \sin n\theta + \bar{a}_n r^{-n} \cos n\theta + \bar{b}_n r^{-n} \sin n\theta\right)$$

In practical magnetic applications, scalar potential becomes:

$$\Phi_M = \sum_n \left(a_n r^n \cos n\theta + b_n r^n \sin n\theta\right)$$

with n integral and a_n, b_n a function of geometry.

This gives components of magnetic flux density:

$$B_r = \sum_n \left(n a_n r^{n-1} \cos n\theta + n b_n r^{n-1} \sin n\theta\right) \qquad B_\theta = \sum_n \left(-n a_n r^{n-1} \sin n\theta + n b_n r^{n-1} \cos n\theta\right)$$

Field distribution features of varied multipole magnet

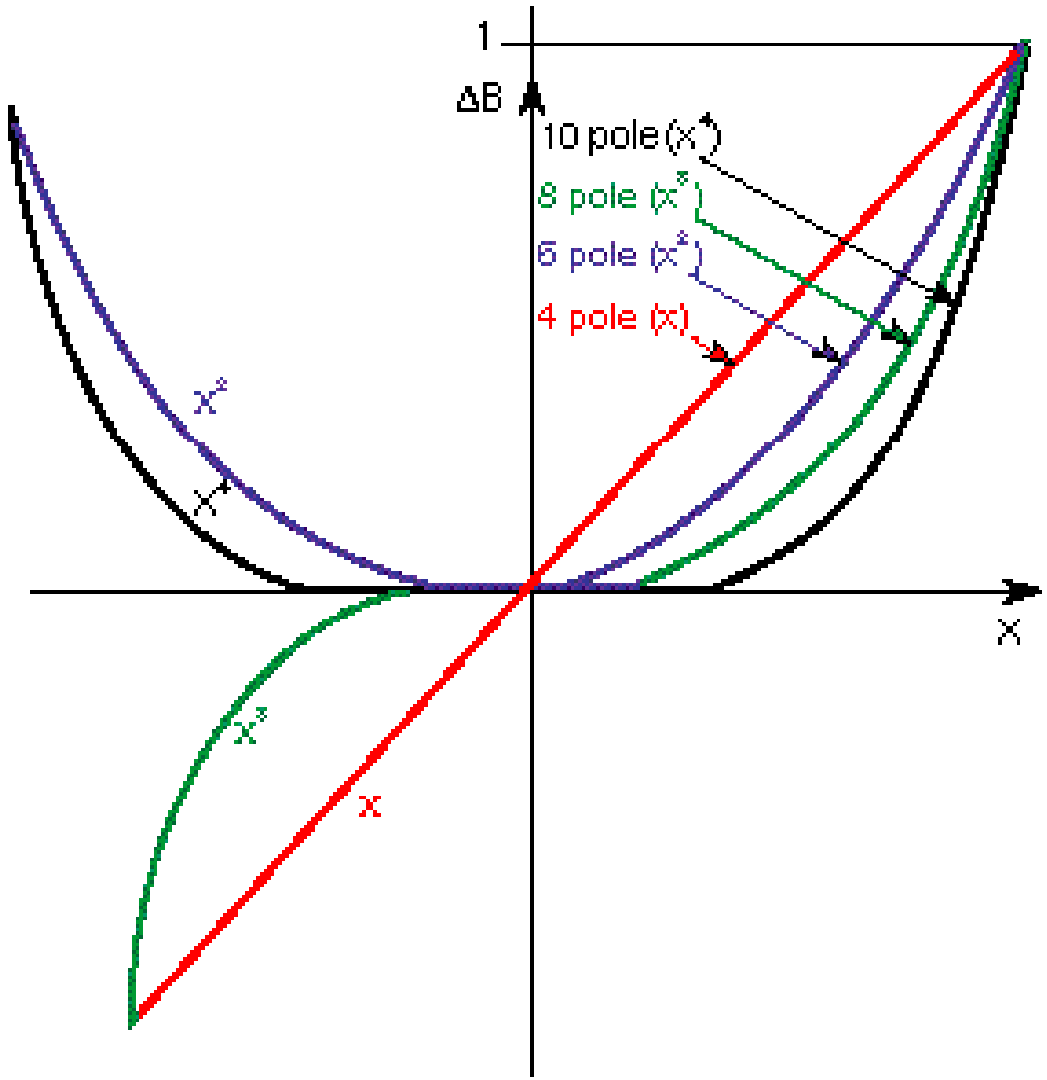

Dipole Magnet-1

- **Dipole field on dipole magnet expressed by n=1 case and and field polarity will be changed when the pole polarity changed. ($\frac{2\pi}{2\times 1}$)**

Cylindrical	Cartesian	
$B_r = a_1 \cos\theta + b_1 \sin\theta$	$B_x = a_1$	$B_x = a_1 + (a_2 + b_2)y$
$B_\theta = -a_1 \sin\theta + b_1 \cos\theta$	$B_y = b_1$	$B_y = b_1 + (a_2 + b_2)x$
$\Phi_M = a_1 r\cos\theta + b_1 r\sin\theta$	$\Phi_M = a_1 x + b_1 y$	$\Phi_M = a_1 x + b_1 y + (a_2 + b_2)xy$

So, $a_1 = 0$, $b_1 \neq 0$ gives vertical dipole field:

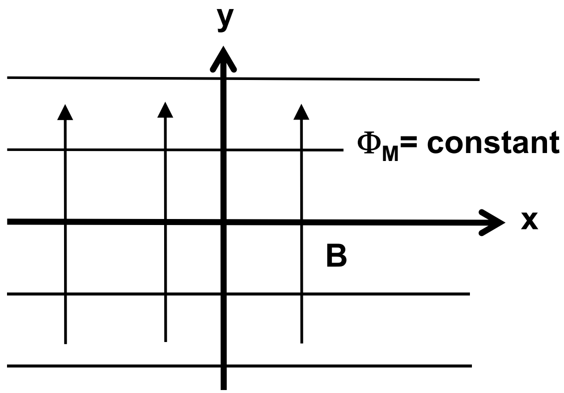

Pure dipole magnet

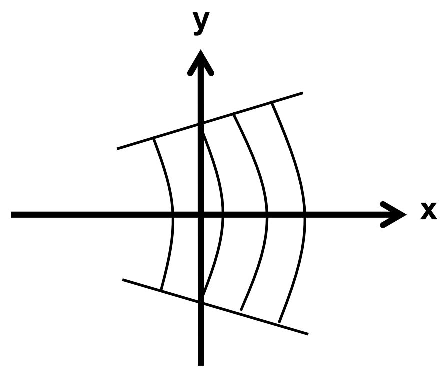

Combine function magnet

Dipole Magnet-2

$b_1 = 0$, $a_1 \neq 0$ gives horizontal dipole field (which is about rotated $\dfrac{\pi}{2 \times 1}$)

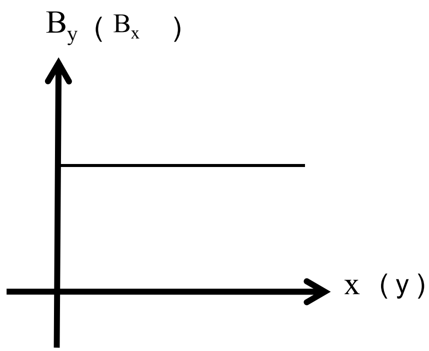

Normal term in separate function dipole

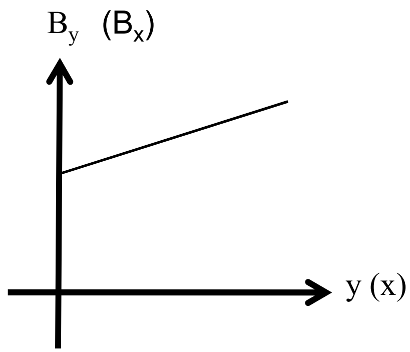

Skew term in combine function dipole

Quadrupole Magnet-1

- **Quadrupole field given by n = 2 case and field polarity will be changed when the pole polarity changed** ΔΘ= =2π /(2 × 2).

Cylindrical	Cartesian
$B_r = 2a_2 r\cos 2\theta + 2b_2 r\sin 2\theta$	$B_x = 2(a_2 x + b_2 y)$
$B_\theta = -2a_2 r\sin 2\theta + 2b_2 r\cos 2\theta$	$B_Y = 2(-a_2 y + b_2 x)$
$\Phi_M = a_2 r^2 \cos 2\theta + b_2 r^2 \sin 2\theta$	$\Phi_M = a_2(x^2 - y^2) + 2b_2 xy$

These are quadrupole distributions, with a_2 = 0 giving 'normal' quadrupole field.

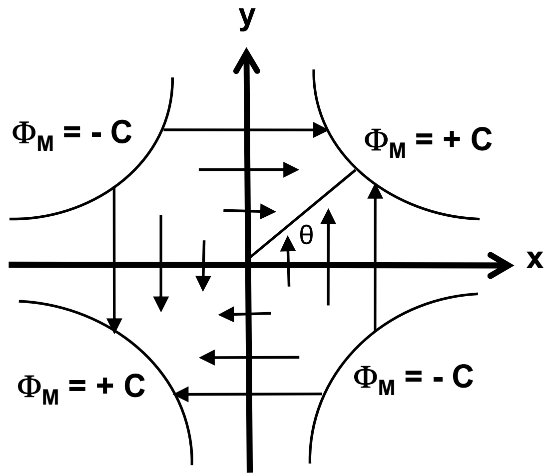

normal

Θ= π /4

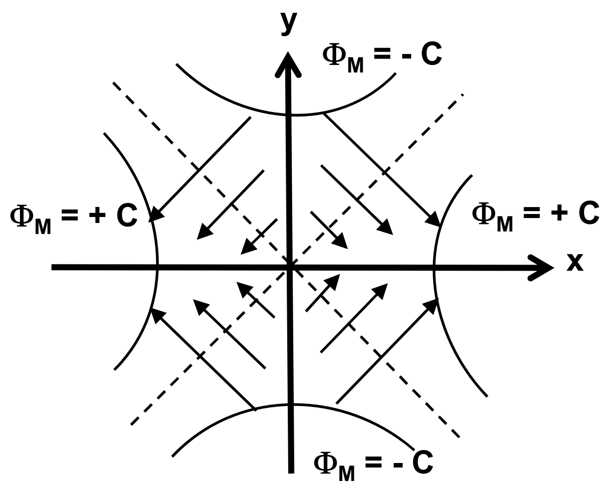

skew

Θ= 0

Quadrupole Magnet-2

Then $b_2 = 0$ gives 'skew' quadrupole fields (which is the above rotated by $\frac{\pi}{2 \times 2}$)

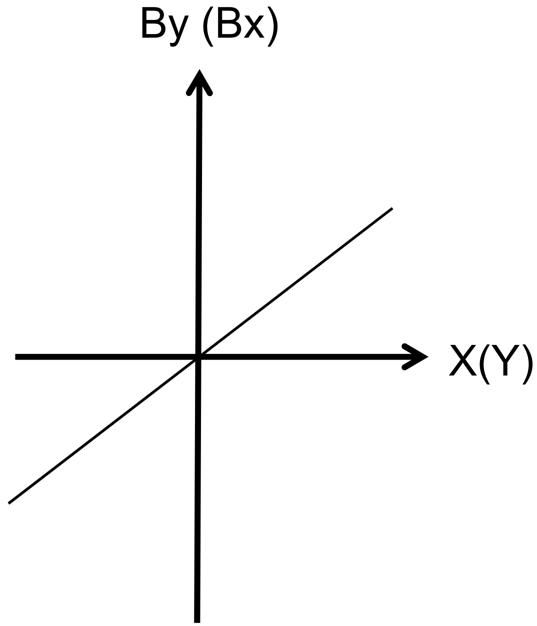

Normal term

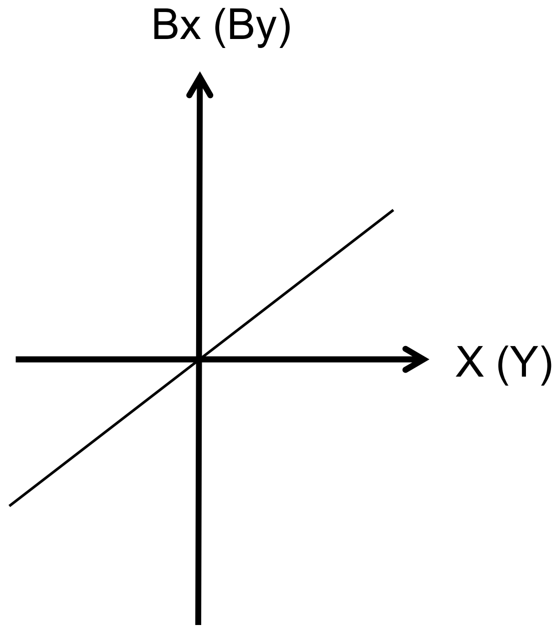

Skew term

Sextupole Magnet-1

- **Sextupole field given by n = 3 case. and field polarity will be changed when the pole polarity changed** ΔΘ= 2π /(3× 2).

Cylindrical	Cartesian
$B_r = 3a_3 r^2 \cos 3\theta + 3b_3 r^2 \sin 3\theta$	$B_x = 3a_3\left(x^2 - y^2\right) + 6b_3 xy$
$B_\theta = -3a_3 r^2 \sin 3\theta + 3b_3 r^2 \cos 3\theta$	$B_y = -6a_3 xy + 3b_3\left(x^2 - y^2\right)$
$\Phi_M = a_3 r^3 \cos 3\theta + b_3 r^3 \sin 3\theta$	$\Phi_M = a_3\left(x^3 - 3y^2 x\right) + b_3\left(3yx^2 - y^3\right)$

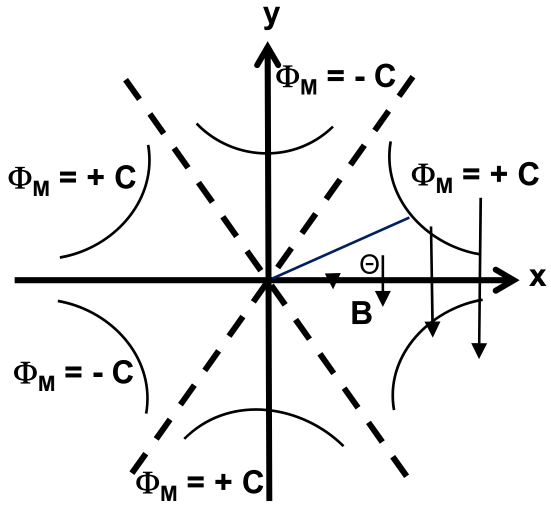

Normal

Θ= π /6

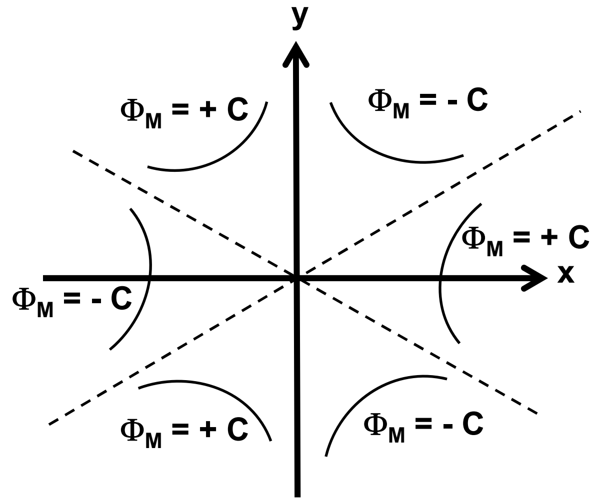

Skew

Θ= 0

Sextupole Magnet-2

For $a_3 = 0$, $b_3 \neq 0$, $B_y \propto x^2$, $B_y = 3b_3\left(x^2 - y^2\right)$ give normal sextupole

For $a_3 \neq 0$, $b_3 = 0$, give skew sextupole (which is about rotated $\frac{\pi}{2 \times 3}$)

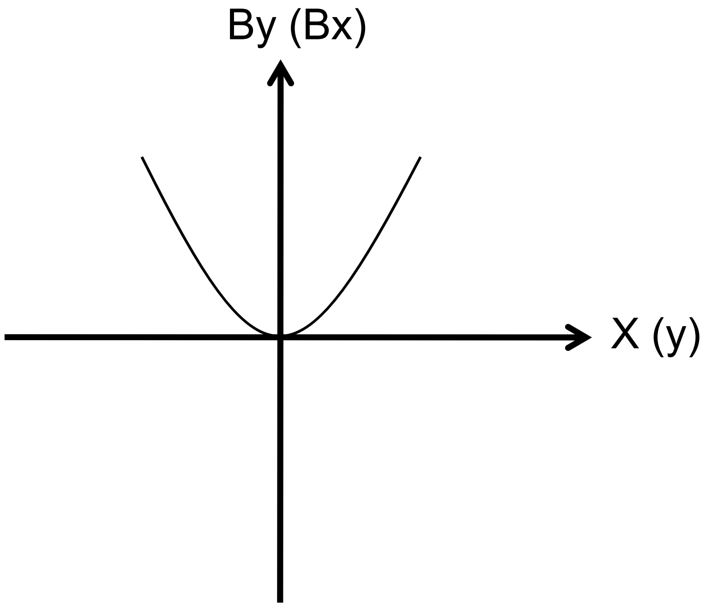

Normal term

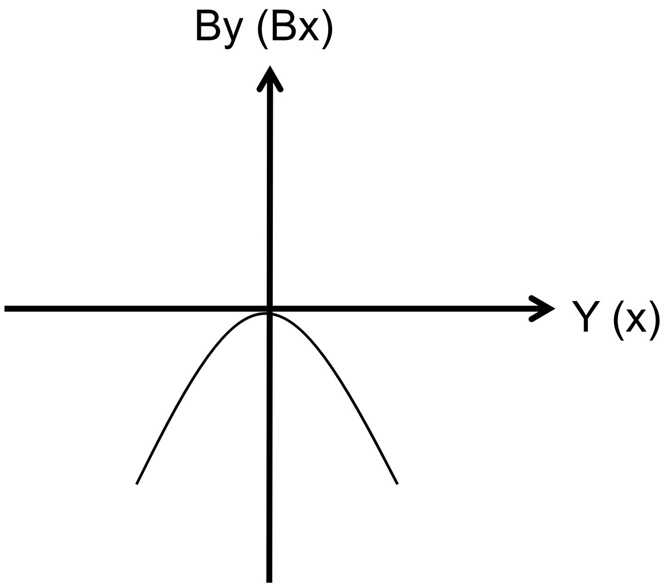

Skew term

Error of dipole magnet

Practical dipole magnet. The shape of the pole surfaces does not exactly correspond to a true straight line and the poles have been truncated laterally to provide space for coils. Skew quadrupole will come from the bad coil.

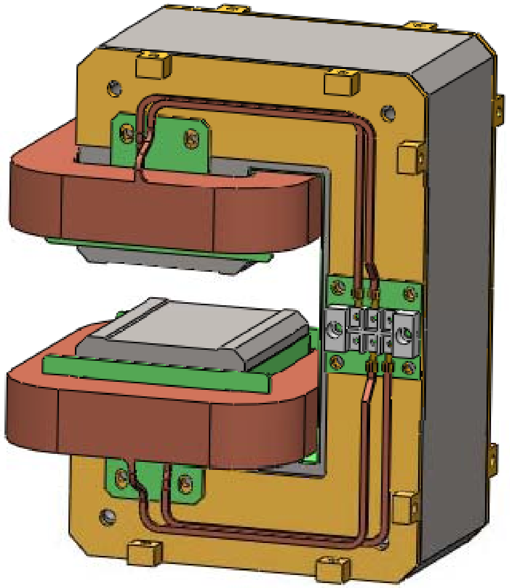

n= 1(2m+1) m=0,1,2,3 -----, n is the allow term for the dipole magnet

(1) Quadrupole (n=2)	: pole tilt or one bad coil	-----Forbidden term
(2) Sextupole (n=3)	: lateral truncation	-----Allow term
(3) Octupole (n=4)	: pole tilt or one bad coil	-----Forbidden term
(4) Decapole (n=5)	: lateral truncation	-----Allow term

Error of quadrupole magnet

Practical quadrupole. The shape of the pole surfaces does not exactly correspond to a true hyperbola and the poles have been truncated laterally to provide space for coils.

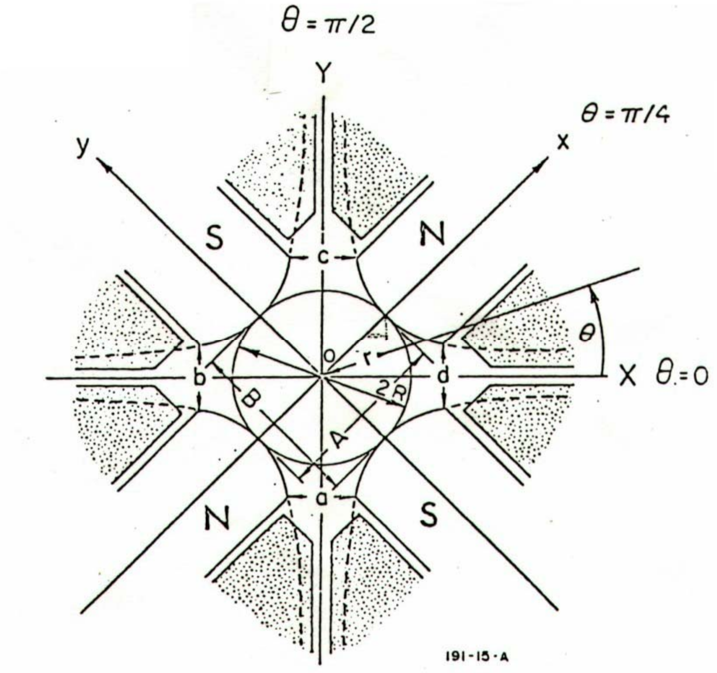

n= 2(2m+1) m=0,1,2,3 -----, n is the allow term for the quadrupole magnet

(1) Sextupole (n=3)	: a=b=c≠d, or one bad coil	-----Forbidden term
(2) Octupole (n=4)	: A=B, a=d, b=c, but a≠b	-----Forbidden term
(3) Decapole (n=5)	: Tilt one pole piece	-----Forbidden term
(4) Dodecapole (n=6)	: a. lateral truncation b. a=b=c=d, A=B≠2R	-----Allow term
(5) 20-pole (n=10)	: a. lateral truncation b. a=b=c=d, A=B≠2R	-----Allow term

Error of sextupole magnet

n= 3(2m+1) m=0,1,2,3 -----, n is the allow term for the sextupole magnet

If dipole field (n=1) changed, the field for the allow term of dipole (n=2m+1) would also be changed.

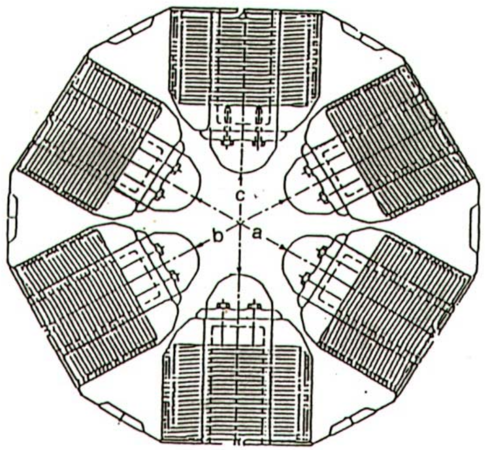

The dipole perturbation in a sextupole field generated by geometrical asymmetry (a=b<c).

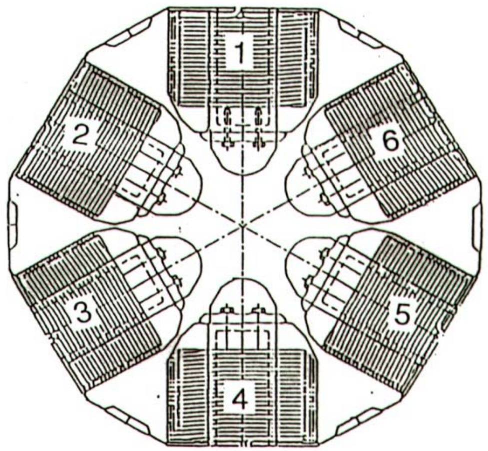

The dipole and skew octupole perturbation in a sextupole field generated by the bad coil (1 and 4 is bad).

(1) Octupole (n=4)	: a=b≠c, or one pair coil bad	-----Forbidden term
(2) Decapole (n=5)	: a=b=c≠2R	-----Forbidden term
(3) 18-pole (n=9)	: a. lateral truncation b. a=b=c≠2R	-----Allow term
(4) 30-pole (n=15)	: a. lateral truncation b. a=b=c≠2R	-----Allow term

Sextupole magnet with corrector mechanism

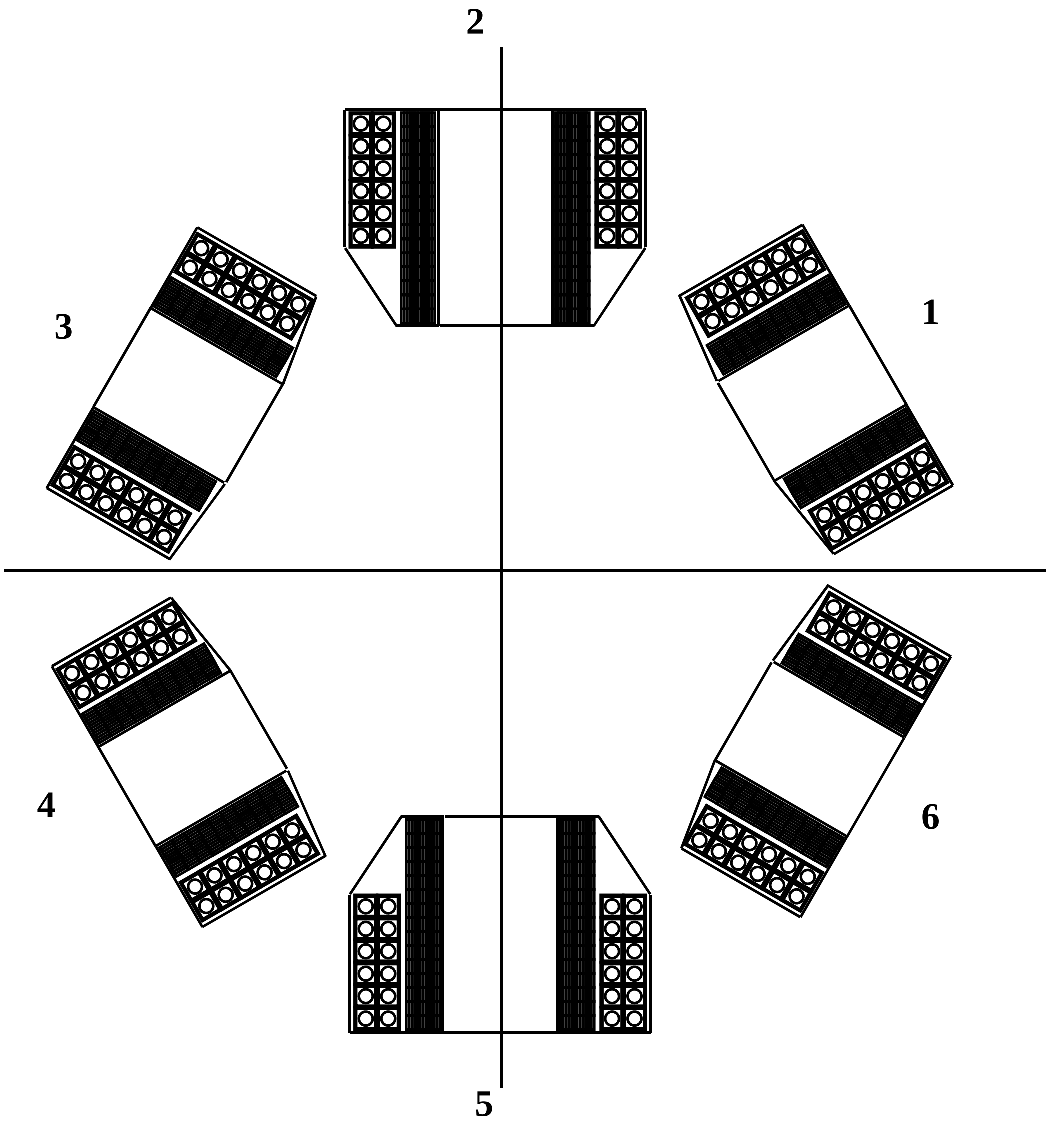

(1) Horizontal corrector (vertical field):
2N turns of Coil 2 & 5 combine together with N turns of Coil 3 & 4 & 1& 6.

(2) Vertical corrector (horizontal field):

N turns of Coil 1 & 6 combine together with N turns of Coil 3 & 4.

(3) Skew quadrupole corrector:
N turns of Coil 2 & 5.

Symmetry constraints in normal dipole, quadurpole and sextupole geometries

Magnet	Symmetry	Constraint
Dipole	$\phi(\theta) = -\phi(2\pi-\theta)$	All $a_n = 0$;
	$\phi(\theta) = \phi(\pi-\theta)$	b_n non-zero only for: $n=(2j-1)=1,3,5,etc$; $(2n)$
Quadrupole	$\phi(\theta) = -\phi(\pi-\theta)$	$b_n = 0$ for all odd n;
	$\phi(\theta) = -\phi(2\pi-\theta)$	All $a_n = 0$;
	$\phi(\theta) = \phi(\pi/2-\theta)$	b_n non-zero only for: $n=2(2j-1)=2,6,10,etc$; $(2n)$
Sextupole	$\phi(\theta) = -\phi(2\pi/3-\theta)$	$b_n = 0$ for all n not multiples of 3;
	$\phi(\theta) = -\phi(4\pi/3-\theta)$	
	$\phi(\theta) = -\phi(2\pi-\theta)$	All $a_n = 0$;
	$\phi(\theta) = \phi(\pi/3-\theta)$	b_n non-zero only for: $n=3(2j-1)=3,9,15,etc.$ $(2n)$

Ideal pole shapes are equal magnetic line

At the steel boundary, with no currents in the steel: $\vec{\nabla} \times \vec{H} = 0$

Apply Stoke's theorem to a closed loop enclosing the boundary:

$$\iint \left(\vec{\nabla} \times \vec{H}\right) \cdot d\vec{S} = \oint \vec{H} \cdot d\vec{\ell}$$

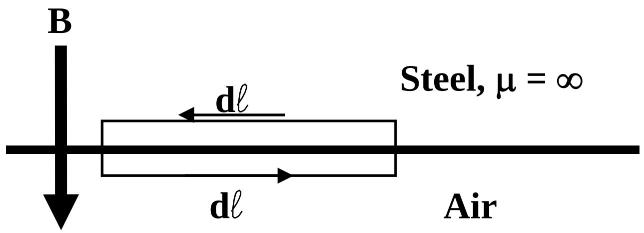

Hence around the loop:

$$\oint \vec{H} \cdot d\vec{\ell} = 0$$

But for infinite permeability in the steel: H = 0;

Therefore outside the steel H = 0 parallel to the boundary.

Therefore B in the air adjacent to the steel is normal to the steel surface at all points on the surface should be equal. Therefore from $\vec{B} = -\vec{\nabla}\Phi_M$, the steel surface is an iso-scalar-potential line.

Contour equations of ideal pole shape

For normal (ie not skew) fields pole profile:

Dipole:

$y = \pm g/2$; (g is interpole gap).

Quadrupole:

$xy = \pm R^2/2$; (R is inscribed radius).

This is the equation of hyperbola which is a natural shape for the pole in a quadrupole.

Sextupole:

$3x^2y - y^3 = \pm R^3$ (R is inscribed radius).

Ampere-turns in a dipole

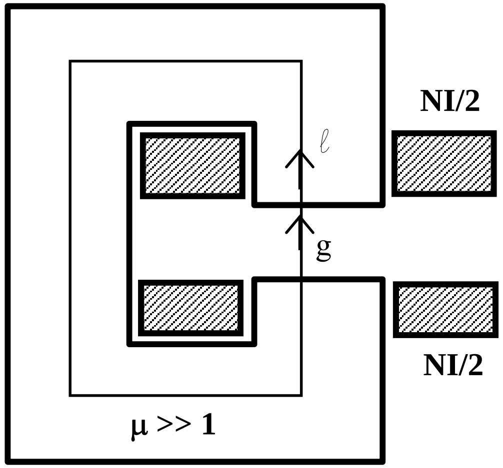

B is approx constant round loop l & g,

and $\quad H_{iron} = H_{air} / \mu;$

$\quad B_{air} = \mu_0 NI / (g + l/\mu);$

g, and l/μ are the reluctance of the gap and the iron.

Ignoring iron reluctance:

$$NI = B g / \mu_0$$

Ampere-turns in quadrupole magnet

Quadruple has pole equation: $\mathrm{xy} = \mathrm{R}^2 / 2$

On x axes

$B_y = G\,x$,

G is gradient (T/m).

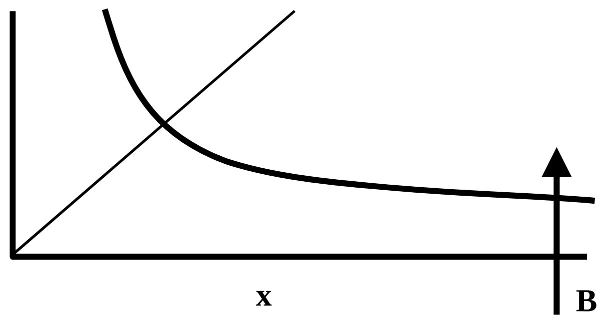

At large x (to give vertical field B):

$$NI = B \cdot \ell / \mu_0 = (\mathrm{G}\ x)(R^2 / 2x)/ \mu_0$$

ie

$$NI = \mathrm{G}\ R^2 / 2\mu_0 \qquad \text{(per pole)}$$

Ampere-turns in sextupole magnet

Sextupole has pole equation:

$$3x^2y - y^3 = \pm R^3$$

On x axes

$B_y = G_s x^2$, G_s is sextupole strength (T/m^2).

At large x (to give vertical field):

$$NI = B \cdot \ell / \mu_0 = \mathrm{Gs}\, x^2 \cdot \left(\frac{R^3}{3x^2 \mu_0} \right) = \frac{\mathrm{Gs}\, R^3}{3\mu_0}$$

Judgment method of field quality

For central pole region:

Dipole: calculate and plot $\frac{B_y(x)-B_y(0)}{B_y(x)}$ in pure dipole or $\frac{B_y(x)-(B_y(0)+g\ x)}{B_y(x)}$ in combine function dipole magnet, g is gradient field in dipole magnet

Quadrupole: calculate and plot $\frac{\mathrm{dB_y(x)}}{\mathrm{dx}}=\mathrm{g(x)}$ and $\frac{B_y(x)-[b_o+b_1x]}{B_y(x)}$ and $\frac{\mathrm{g(x)-g(0)}}{\mathrm{g(0)}}$

Sextupole: calculate and plot $\frac{\mathrm{d^2B_y(x)}}{\mathrm{dx^2}}=\mathrm{S(x)}$ and $\frac{B_y(x)-[b_o+b_1x+b_2x^2]}{B_y(x)}$ and $\frac{\mathrm{S(x)-S(0)}}{\mathrm{S(0)}}$

For integral good field region:

Dipole: $\frac{\int B_y(x)ds-\int B_y(0)ds}{\int B_y(x)ds}$ or $\frac{\int B_y(x)ds-\left[\int B_y(0)ds+\int gxds\right]}{\int B_y(x)ds}$

Quadurpole: $\frac{\int B(x)ds-[\int(b_o+b_1x)ds]}{\int B(x)ds}$ and $\frac{\int g(x)ds-\int g(0)ds}{\int g(0)ds}$

Sextuple: $\frac{\int B(x)ds-[\int(b_o+b_1x+b_2x^2)ds]}{\int B(x)ds}$ and $\frac{\int \mathrm{S(x)ds}-\int \mathrm{S(0)ds}}{\int \mathrm{S(0)ds}}$

Magnet geometries and pole shim of dipole magnet

'C' Type:

Advantages:
- Easy access for installation;
- Classic design for field measurement;

Disadvantaged:
- Pole shims needed;
- Asymmetric (small);
- Less rigid;

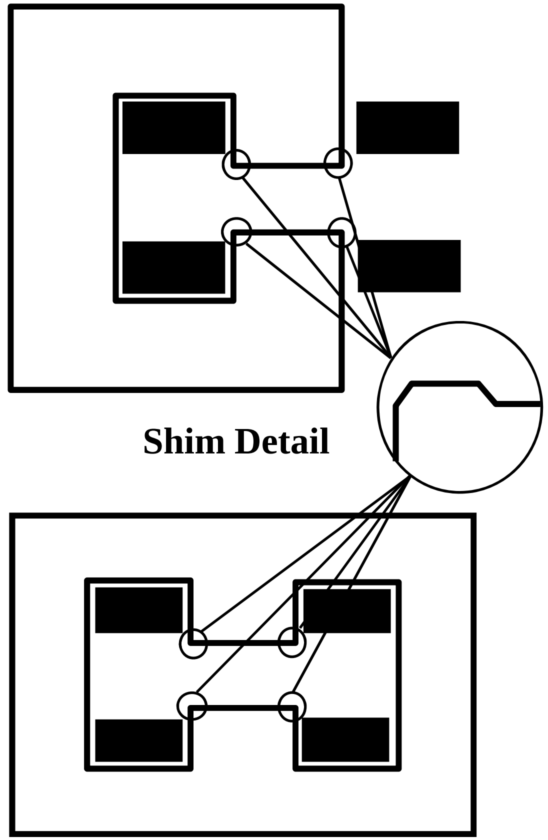

'H' Type:

Advantages:
- Symmetric of field features;
- More rigid;

Disadvantages:
- Also needs shims;
- Access problems for installation.
- Not easy for field measurement.

Magnet geometries and pole shim of multipole magnet

Quadrupole and Sextupole Type:

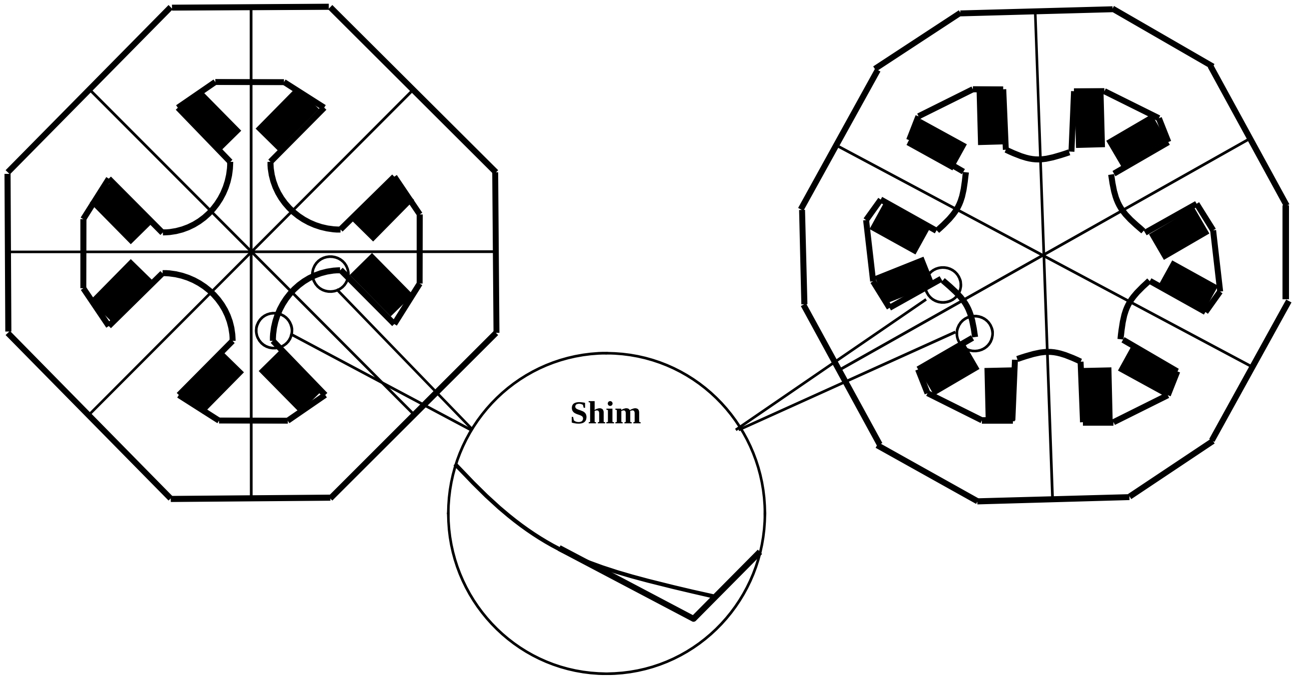

However, shim design should consider the assembly accuracy and the engineering factor

Effect of shim and pole width on distribution

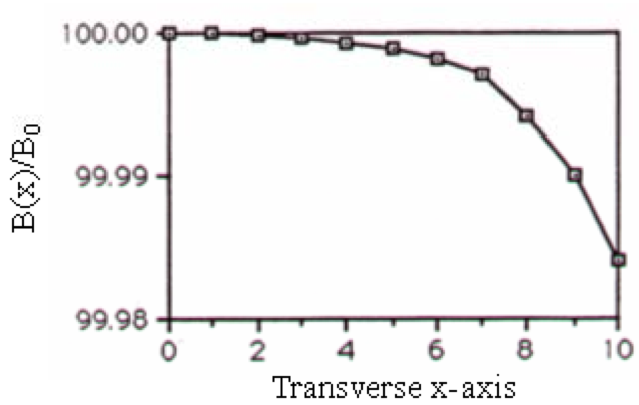

Very large pole, no shim

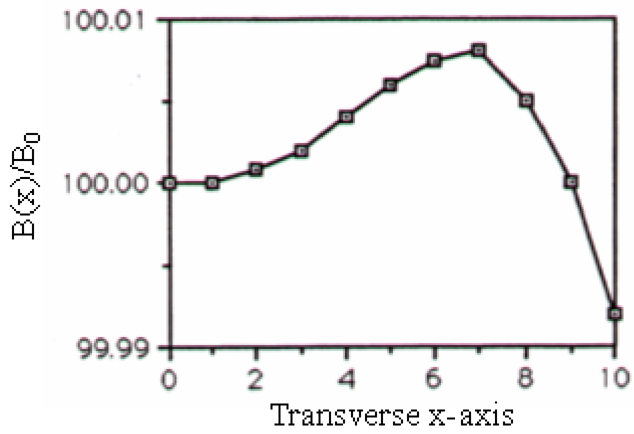

Large pole, small shim

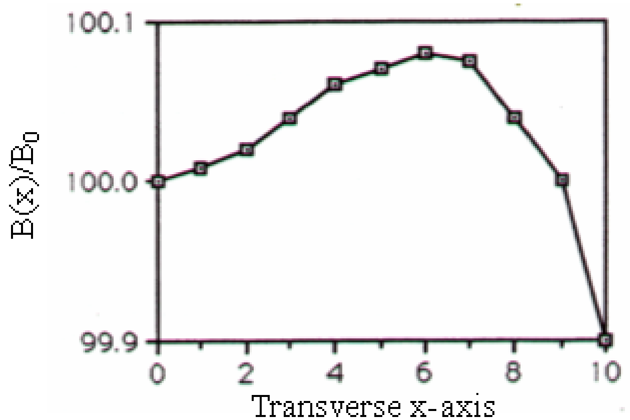

Smaller pole, large shim

Magnet chamfer for avoiding field saturation at magnet edge

- Chamfering at both sides of dipole magnet to compensate for the sextupole components and the allow harmonic terms.

- Chamfering at both sides of the magnet edge to compensate for the 12-pole (18-pole) on quadrupole (sextupole) magnets and their allow harmonic terms.

- Chamfering means to cut the end pole along 45° on the longitudinal axis (z-axis) to avoid the field saturation at magnet edge.

Square ends

* display non linear effects (saturation);
* give no control of radial distribution in the fringe region.

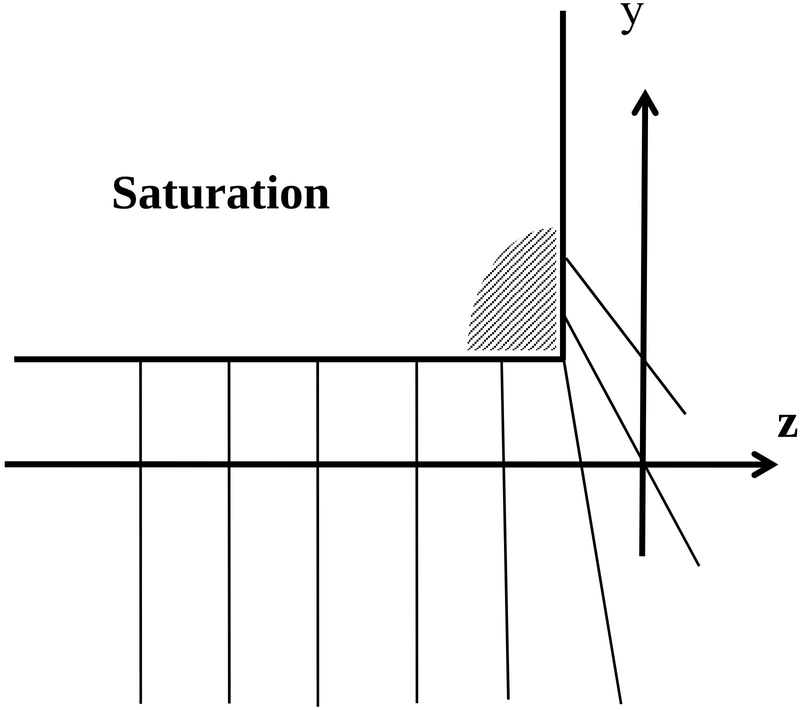

Chamfered ends or shim ends

* define magnetic length more precisely;

* prevent saturation;

* control transverse distribution;

* prevent flux entering iron normal to lamination (vital for ac magnets).

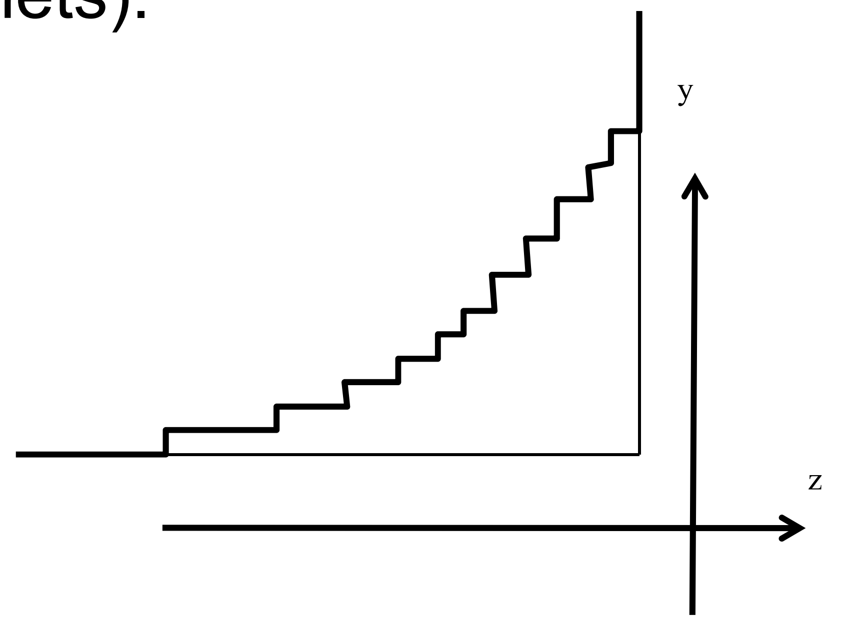

Comparison of four commonly used magnet computation codes

Advantages	Disadvantages
MAGNET:	
* Quick to learn, simple to use; * Small(ish) cpu use; * Fast execution time;	* Only 2D predictions; * Batch processing only-slows down problem turn-round time; * Inflexible rectangular lattice; * Inflexible data input; * Geometry errors possible from interaction of input data with lattice; * No pre or post processing; * Poor performance in high saturation;
POISSON:	
* Similar computation as MAGNET; * Interactive input/output possible; * More input options with greater flexibility; * Flexible lattice eliminates geometery errors; * Better handing of local saturation; * Some post processing available.	* Harder to learn; * Only 2D predictions.

Comparison of four commonly used magnet computation codes

Advantages	Disadvantages
TOSCA:	
* Full three dimensional package; * Accurate prediction of distribution and strength in 3D; * Extensive pre/post-processing; * Multipole function calculation * For static & DC & AC field calculation * Run in PC or workstation	* Training course needed for familiarization; * Expensive to purchase; * Large computer needed. * Large use of memory. * Cpu time is hours for non-linear 3D problem.
RADIA:	
* Full three dimensional package * Accurate prediction of distribution and strength in 3D * With quick-time to view and rotat 3D structure * Easy to build model with mathematic * Fast calculation & data analysis * Run in PC or MAC	* Larger computer needed; * Large use of memory; * Careful to make the segmentation; * DC field calculation; * Can down load from ESRF ID group website.

Field calculation by Tosca code

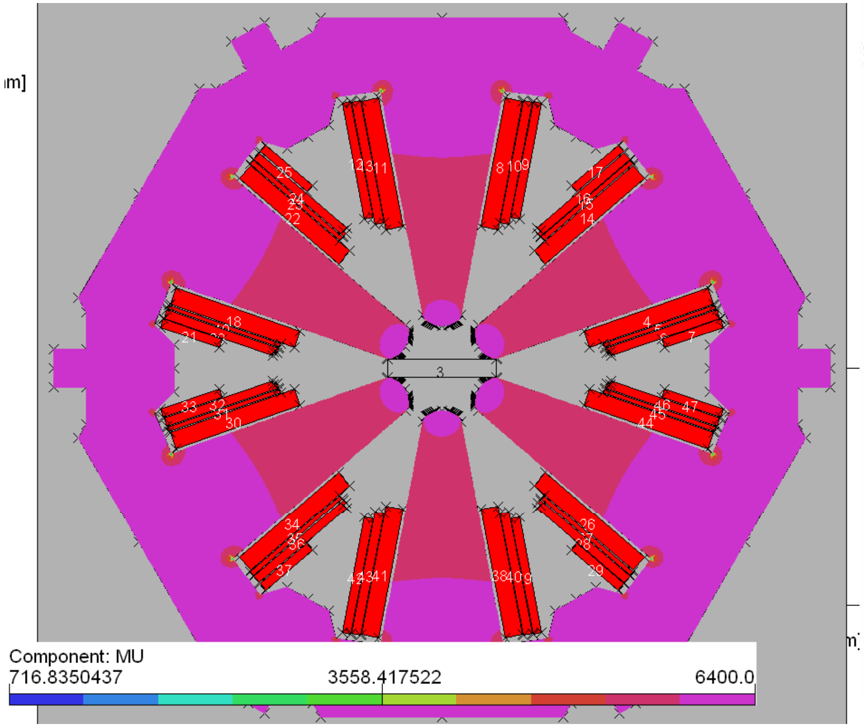

Without trim coil charging

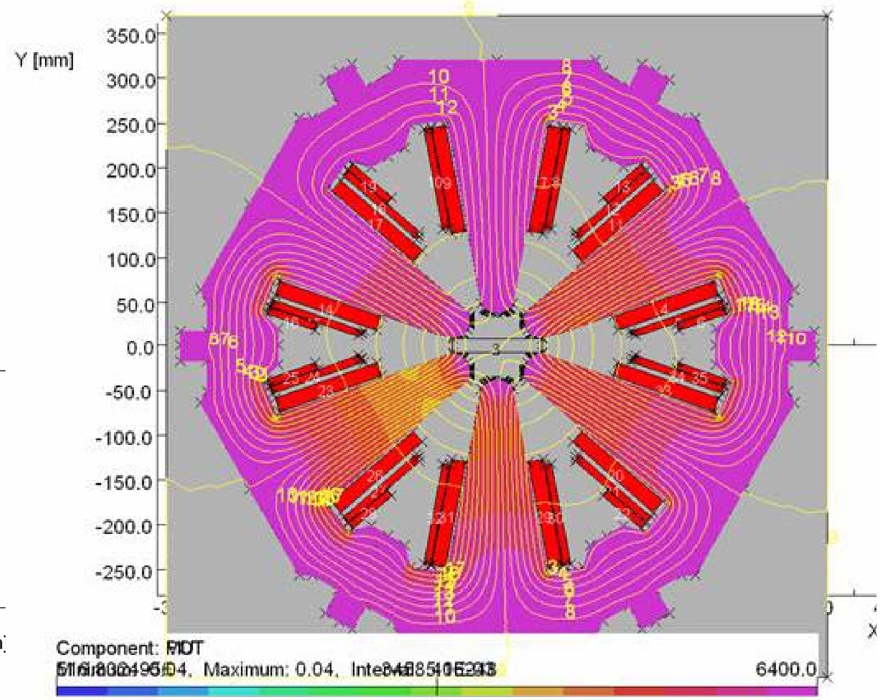

With trim coil charging

- Magnet pole and return yoke should be large enough to avoid field saturation
- The maximum current density is within 1 A/mm^2 of the corrector on the sextupole magnet

AC&DC Corrector design

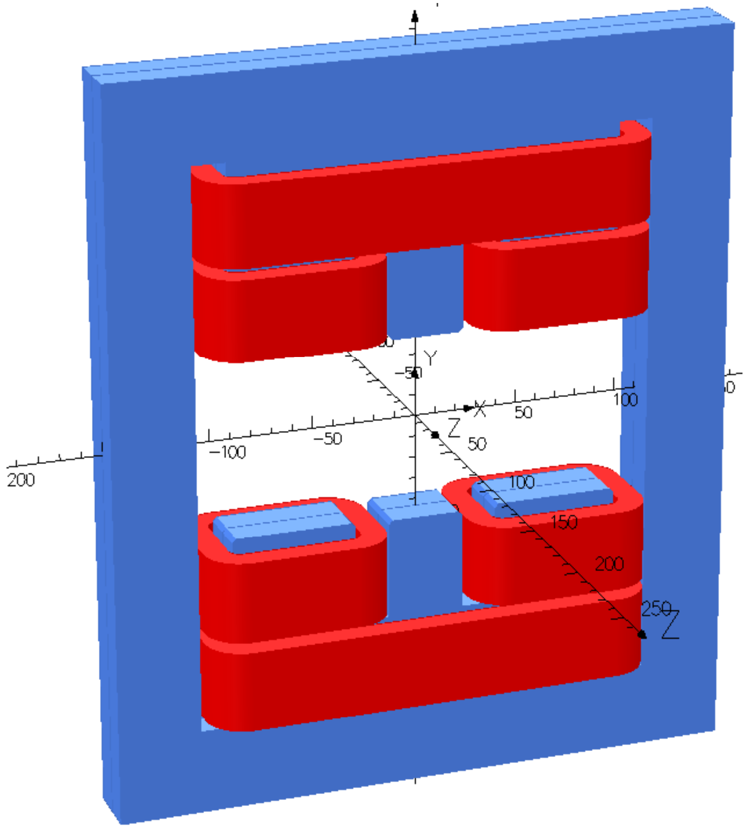

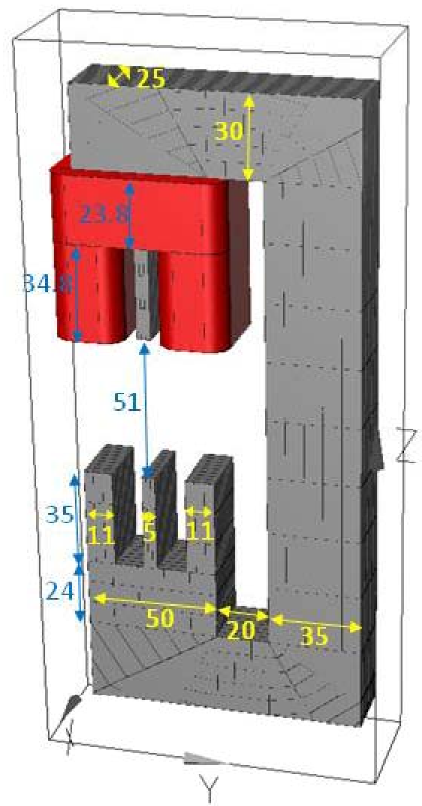

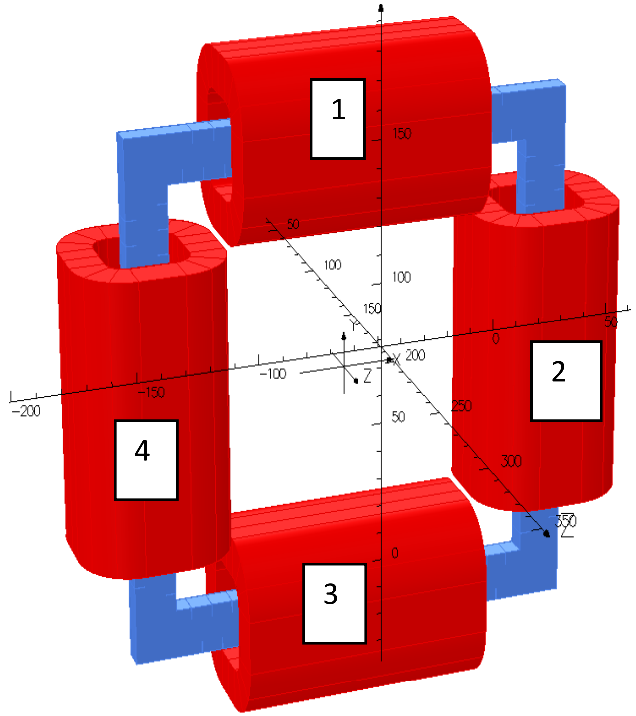

$I(t)=I_0 Sin(\omega t)$

$$P = i(t)\times V = i(t)\times[L\times\frac{di(t)}{dt} + i(t)\times R]$$

$$\text{Average power} = P_{average} = \sqrt{\frac{1}{T}\int_0^T P^2(t)dt}$$

AC corrector

$I(t)=I_0$

$$P = i(t)\times V = i(t)\times i(t)\times R$$

DC corrector

Dipole shim or chamfer Effect

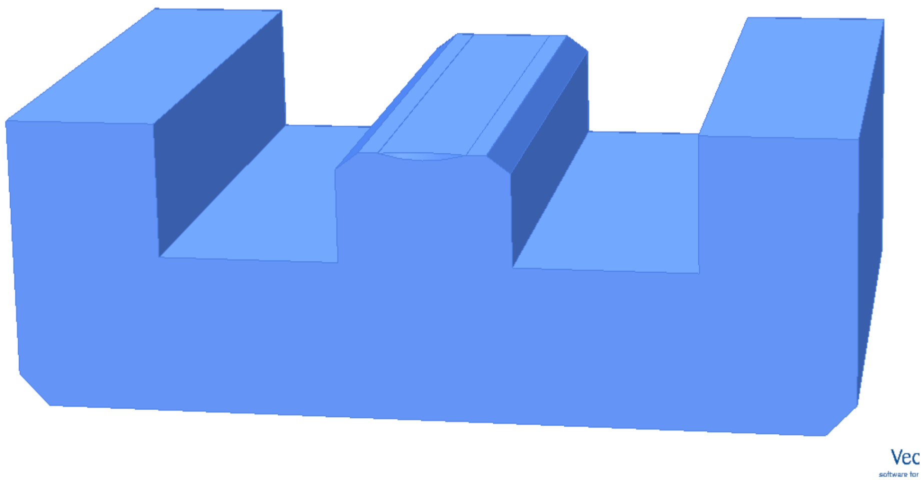

Chamfer

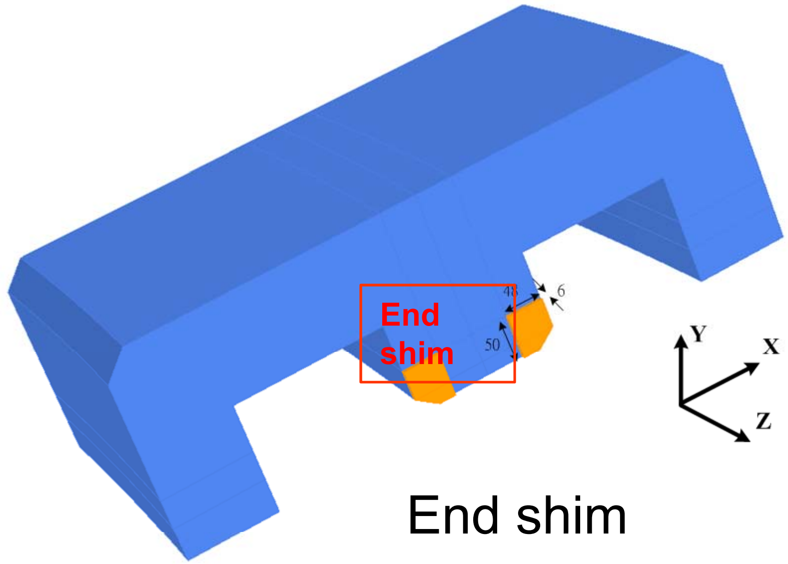

End shim

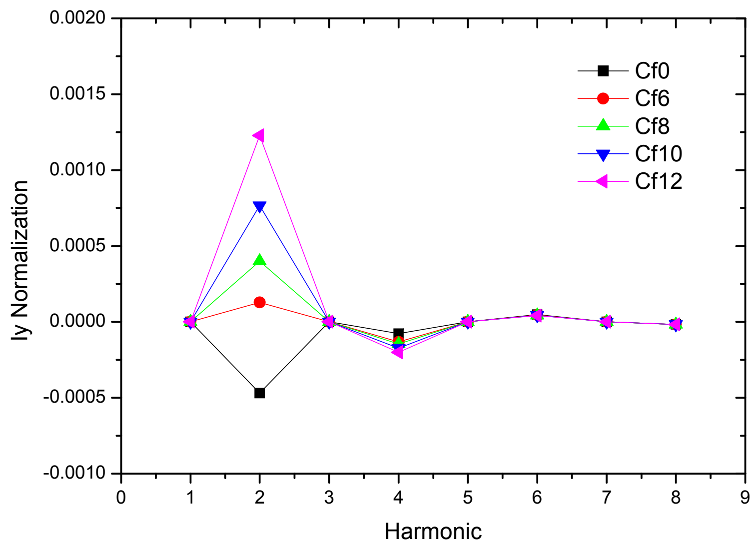

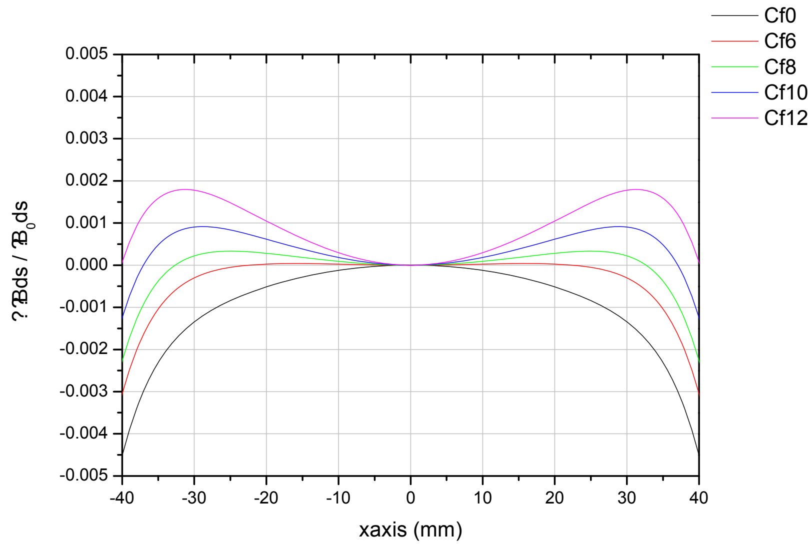

Field analysis of dipole magnet

Lamination mapping

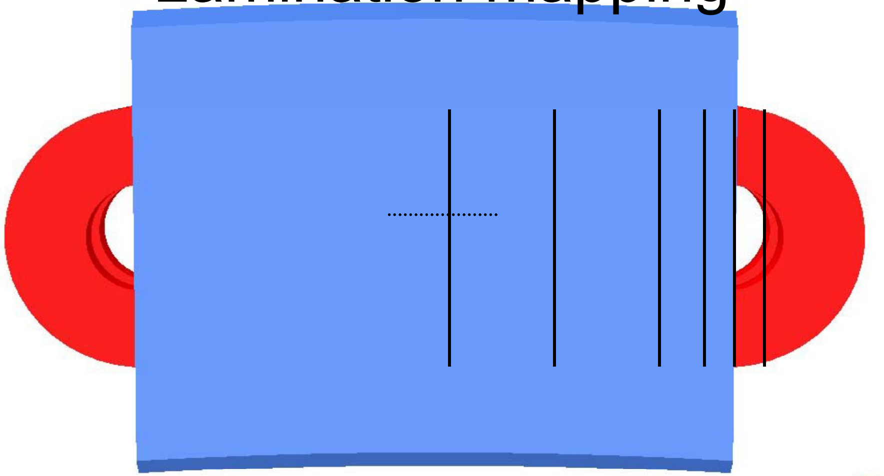

Radial mapping

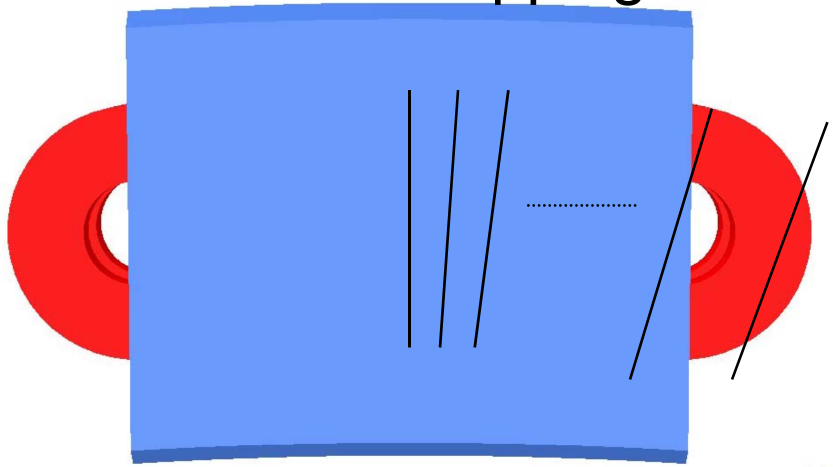

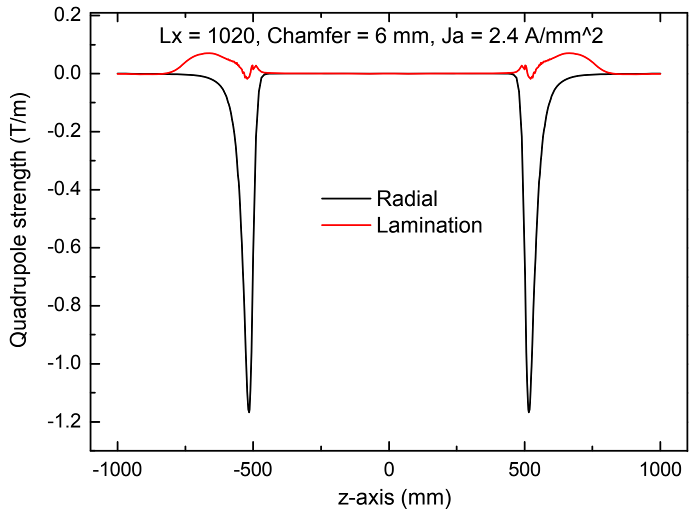

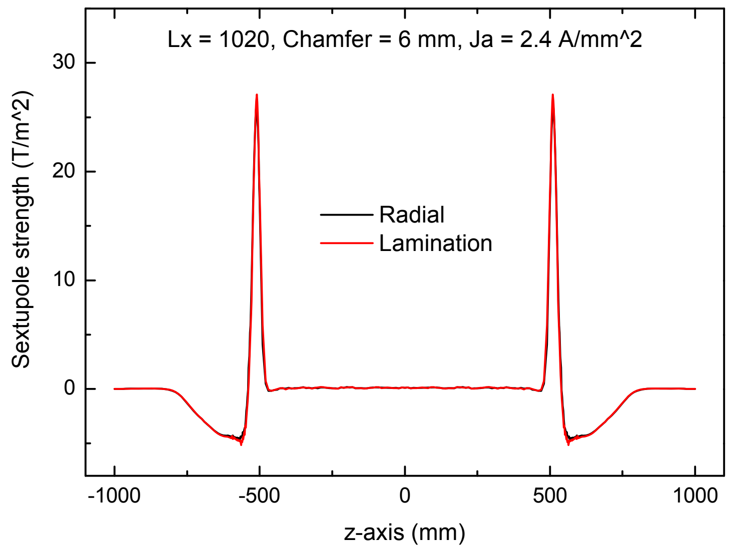

- The weak edge focus strength is around 0.026 T (0.0026 m^{-1})

Quadrupole&sextupole magnet chamfer effect

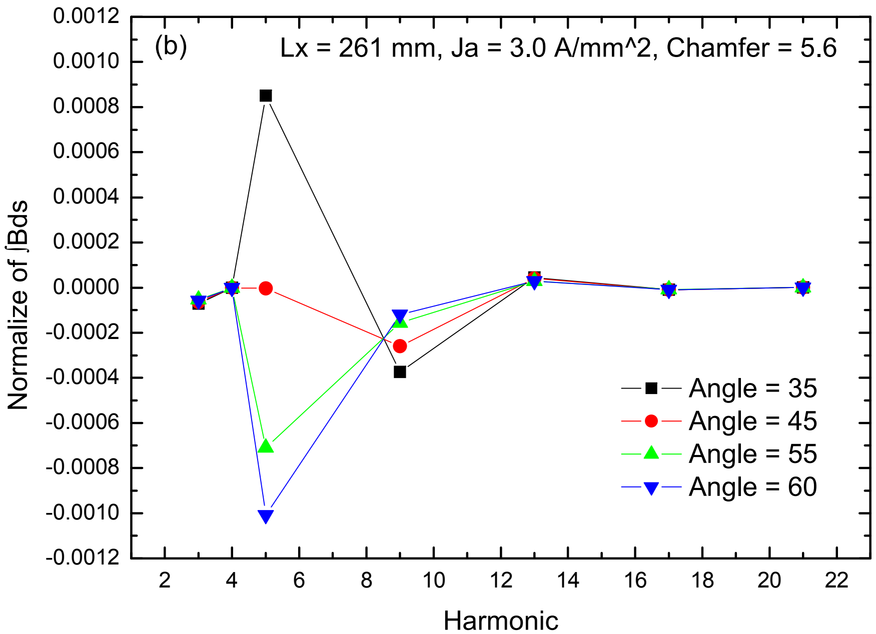

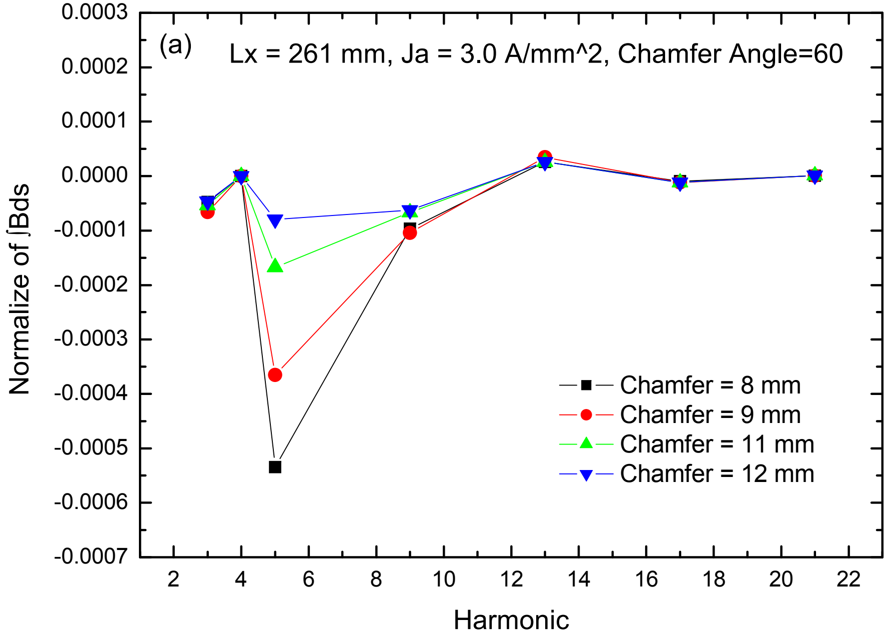

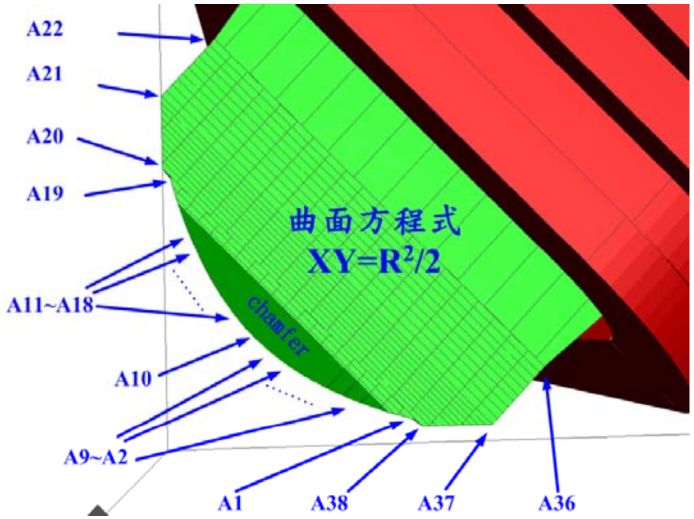

Quadrupole magnet

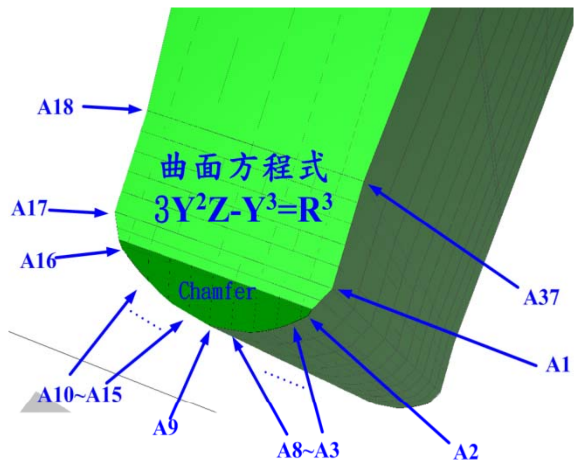

Sextupole magnet

Quadrupole chamfered ends or shim ends effect

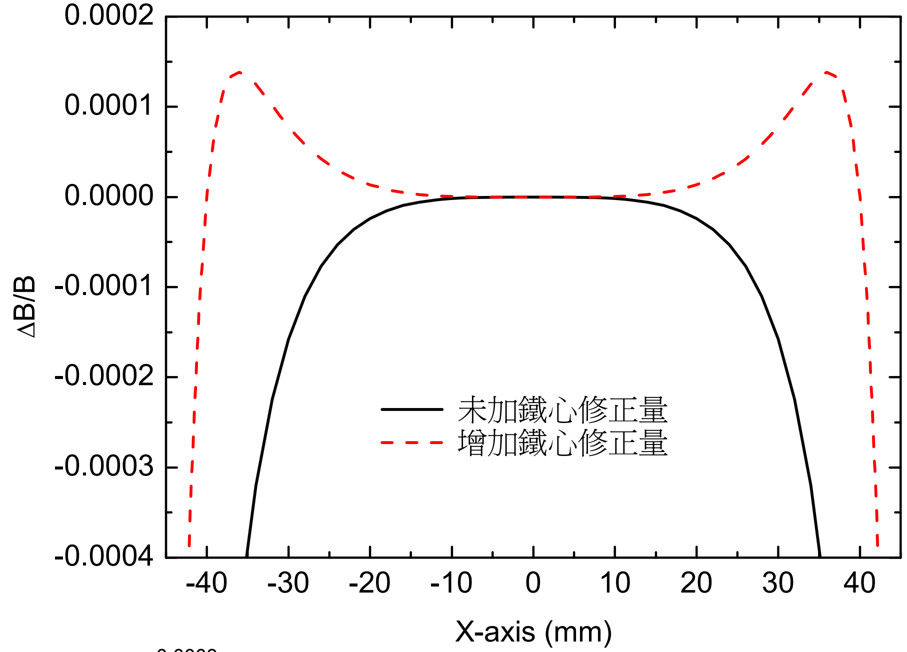

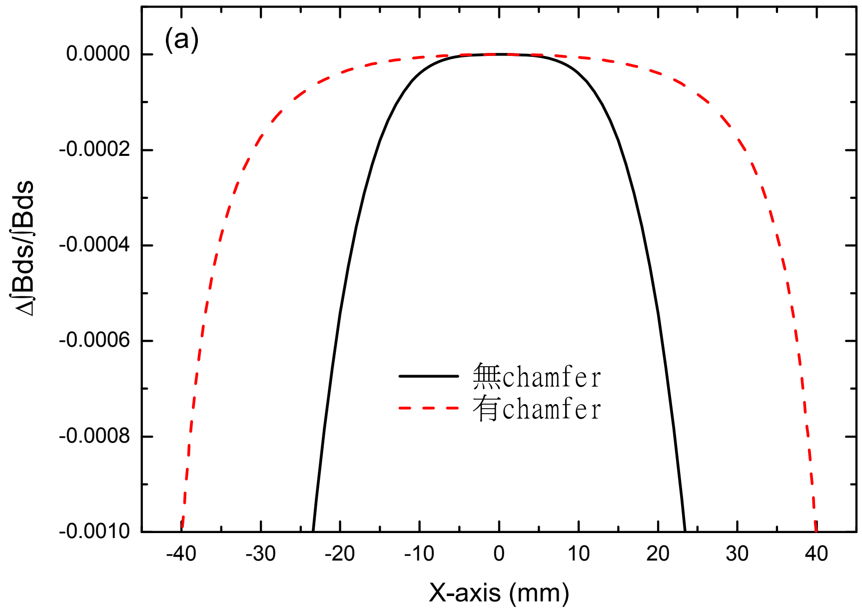

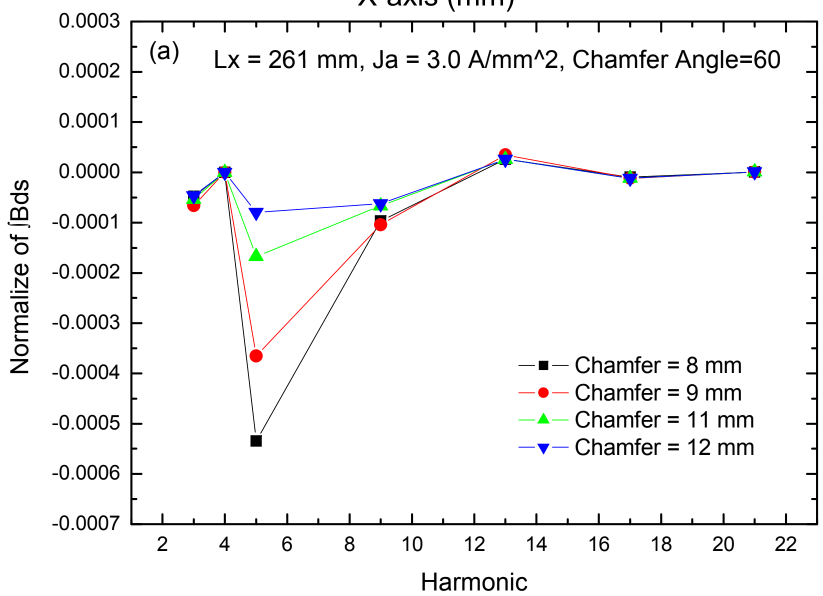

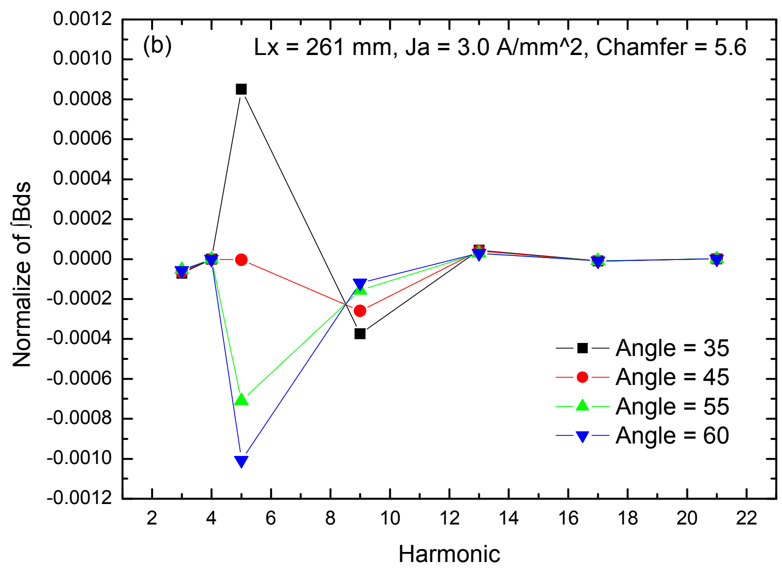

Quadrupole field analysis by FFT method

File path

D:\jwchen\3D_model_4\4pole_1\3D\q20070508_block_length285_chamfer_5mm_int_Ro.txt

Source of data: Opera (three columns) ◉ 不含欄位名稱

○ Data copy

Copy type: 1/4 model

○ Data analysis

Load file

注意事項：
1. 若要修改程式，須注意資料第一點及最後一點的磁場不能相等
2. Data analysis 即為 data 乘上sin(nθ)

Magnet Type: Quadrupole

\# of order: 20

Theta: 360

MeasureRadius: 34.00

NormalizeRadius: 30.00

Process Iy

Raw data Graph

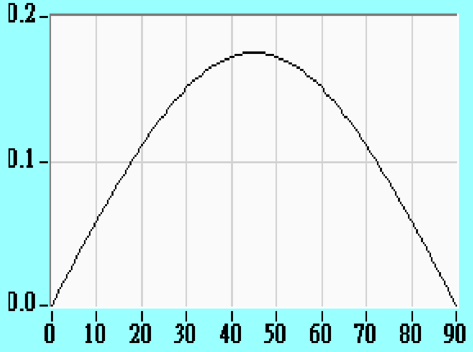

Sort data Graph

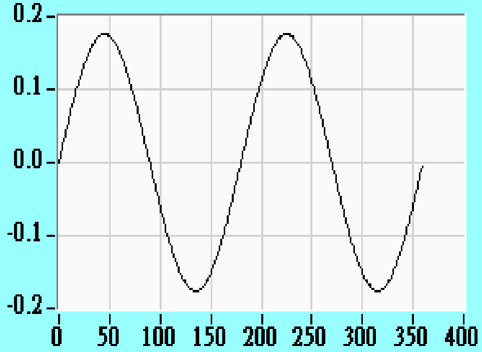

FFT Coefficient

	Ratio (HC1)	Total (C1)	Nor. (HC3)	Skew (a_comp)	Nomal (b_comp)	θ (degree)
0	6.17401E-14	3.42041E-16	7.04951E-14	-2.95799E-16	1.71741E-16	1.49861E+2
1	9.92582E+1	5.49892E-1	1.00000E+2	-1.37584E-17	-5.49892E-1	-9.00000E+1
2	4.52118E-16	2.50474E-18	4.01909E-16	2.06989E-18	-1.41042E-18	-3.42705E+1
3	3.80093E-3	2.10572E-5	2.98131E-3	4.49918E-18	-2.10572E-5	-9.00000E+1
4	1.31992E-14	7.31236E-17	9.13497E-15	-7.30098E-17	4.07681E-18	1.76804E+2
5	7.20967E-1	3.99417E-3	1.70269E-2	-1.39332E-18	3.99417E-3	9.00000E+1
6	3.05313E-14	1.69144E-16	1.64510E-14	1.28496E-16	-1.09993E-16	-4.05637E+1
7	3.31191E-4	1.83480E-6	1.57459E-4	-4.41136E-17	-1.83480E-6	-9.00000E+1
8	1.13411E-20	6.28299E-23	4.75757E-21	0.00000E+0	6.28299E-23	9.00000E+1
9	1.00367E-2	5.56034E-5	3.71503E-3	4.17512E-17	5.56034E-5	9.00000E+1
10	9.97814E-15	5.52790E-17	3.25885E-15	-4.74749E-17	-2.83179E-17	-1.49185E+2
11	1.09695E-3	6.07710E-6	3.16113E-4	-5.62779E-19	6.07710E-6	9.00000E+1
12	6.42384E-15	3.55882E-17	1.63341E-15	-3.39989E-17	1.05164E-17	1.62812E+2
13	3.42378E-3	1.89678E-5	7.68153E-4	-3.15446E-17	-1.89678E-5	-9.00000E+1
14	1.01067E-16	5.59914E-19	2.00076E-17	5.18658E-19	-2.10943E-19	-2.21320E+1
15	6.15457E-4	3.40964E-6	1.07504E-4	5.71294E-17	3.40964E-6	9.00000E+1
16	4.00807E-15	2.22048E-17	6.17738E-16	-2.21460E-17	1.61522E-18	1.75829E+2
17	8.83569E-4	4.89498E-6	1.20158E-4	-7.29790E-19	4.89498E-6	9.00000E+1
18	4.32197E-15	2.39438E-17	5.18603E-16	2.27517E-17	-7.46109E-18	-1.81562E+1
19	6.25168E-4	3.46344E-6	6.61899E-5	-2.31845E-17	3.46344E-6	9.00000E+1

Br×Sin(2θ) Fast Fourier Transform

Sextupole field analysis by FFT method

File path

C:\Mathematica-radia\Sextupole\cykuo\data-cca\angBr(r34ang1)_sextupole-1.TXT

Source of data

Radia (two columns)

不含欄位名稱

Data copy

Copy type

1/4 model

Data analysis

Load file

注意事項：
1. 若要修改程式，須注意資料第一點及最後一點的磁場不能相等
2. Data analysis 即爲 data 乘上sin(nθ)

Magnet Type

Sextupole

# of order

21

Theta

360

MeasureRadius

34.00

NormalizeRadius

30.00

Process Iy

Raw data Graph

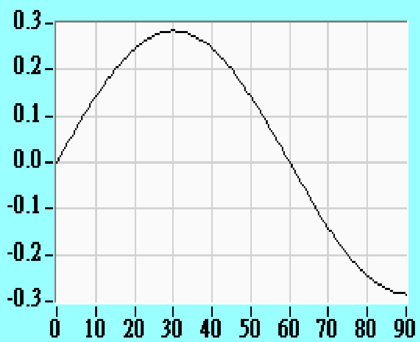

Sort data Graph

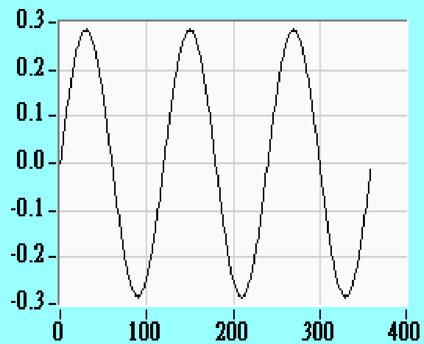

FFT Coefficient

	Ratio (HC1)	Total (C1)	Nor. (HC3)	Skew (a_comp)	Normal (b_comp)	θ (degree)
0	4.5600E-3	4.1221E-5	5.8683E-3	-1.6039E-18	-4.1221E-5	-9.0000E+1
1	0.0000E+0	0.0000E+0	0.0000E+0	0.0000E+0	0.0000E+0	0.0000E+0
2	9.9809E+1	9.0224E-1	1.0000E+2	6.3029E-17	-9.0224E-1	-9.0000E+1
3	0.0000E+0	0.0000E+0	0.0000E+0	0.0000E+0	0.0000E+0	0.0000E+0
4	2.4609E-3	2.2246E-5	1.9196E-3	-1.7589E-18	2.2246E-5	9.0000E+1
5	0.0000E+0	0.0000E+0	0.0000E+0	0.0000E+0	0.0000E+0	0.0000E+0
6	5.2250E-3	4.7232E-5	3.1731E-3	-7.5278E-19	4.7232E-5	9.0000E+1
7	0.0000E+0	0.0000E+0	0.0000E+0	0.0000E+0	0.0000E+0	0.0000E+0
8	1.2995E-1	1.1747E-3	6.1440E-2	-1.8613E-19	1.1747E-3	9.0000E+1
9	0.0000E+0	0.0000E+0	0.0000E+0	0.0000E+0	0.0000E+0	0.0000E+0
10	3.6966E-3	3.3416E-5	1.3607E-3	-5.9111E-20	-3.3416E-5	-9.0000E+1
11	0.0000E+0	0.0000E+0	0.0000E+0	0.0000E+0	0.0000E+0	0.0000E+0
12	1.0418E-3	9.4172E-6	2.9856E-4	2.5373E-19	-9.4172E-6	-9.0000E+1
13	0.0000E+0	0.0000E+0	0.0000E+0	0.0000E+0	0.0000E+0	0.0000E+0
14	6.4721E-3	5.8505E-5	1.4441E-3	-1.4691E-17	-5.8505E-5	-9.0000E+1
15	0.0000E+0	0.0000E+0	0.0000E+0	0.0000E+0	0.0000E+0	0.0000E+0
16	1.3714E-3	1.2397E-5	2.3823E-4	2.1479E-18	1.2397E-5	9.0000E+1
17	0.0000E+0	0.0000E+0	0.0000E+0	0.0000E+0	0.0000E+0	0.0000E+0
18	4.8615E-5	4.3946E-7	6.5747E-6	1.3156E-18	4.3946E-7	9.0000E+1
19	0.0000E+0	0.0000E+0	0.0000E+0	0.0000E+0	0.0000E+0	0.0000E+0
20	3.6398E-2	3.2903E-4	3.8324E-3	1.7189E-17	3.2903E-4	9.0000E+1

Br×Sin(3θ) Fast Fourier Transform

B-H function of quadrupole magnet with iron yoke cutting

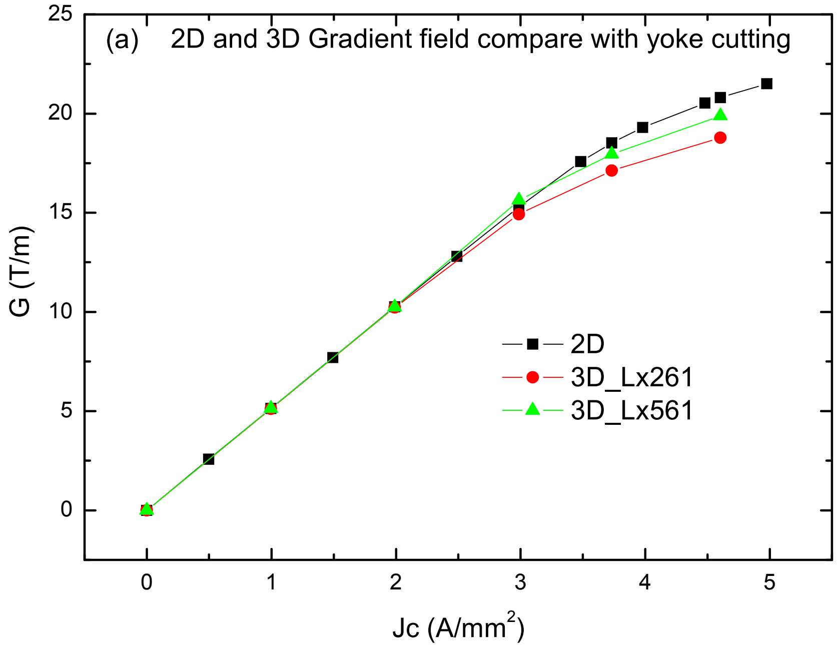

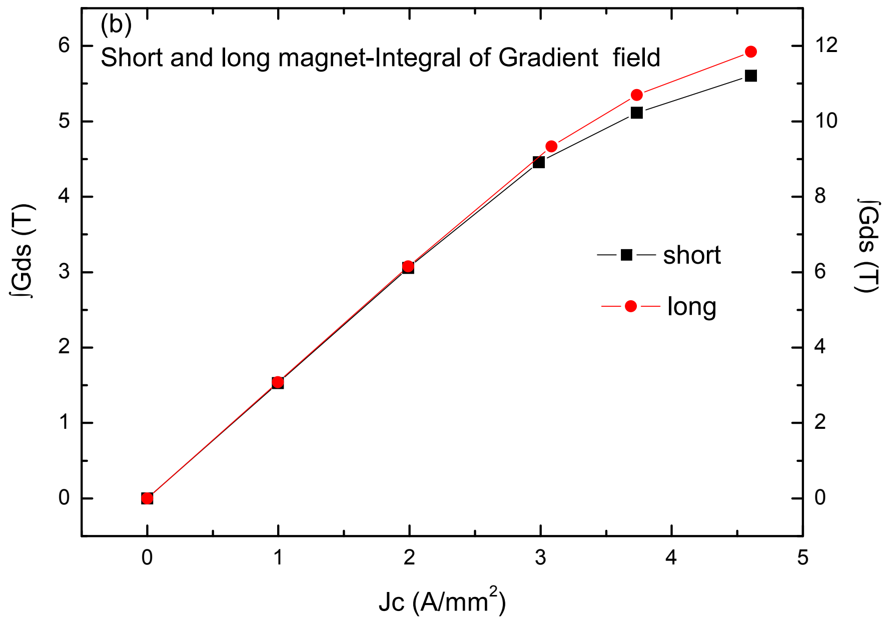

- There is a big difference of the quadrupole field strength between 2D and 3D at high field region
- Saturation had happened with yoke cutting at the nominal field
- Field saturation in the short quadrupole magnet is larger than the long quadrupole magnet
- Operating at 3.5GeV is impossible on the 3D calculation with yoke cutting and without any compensation

Magnet effective length definition

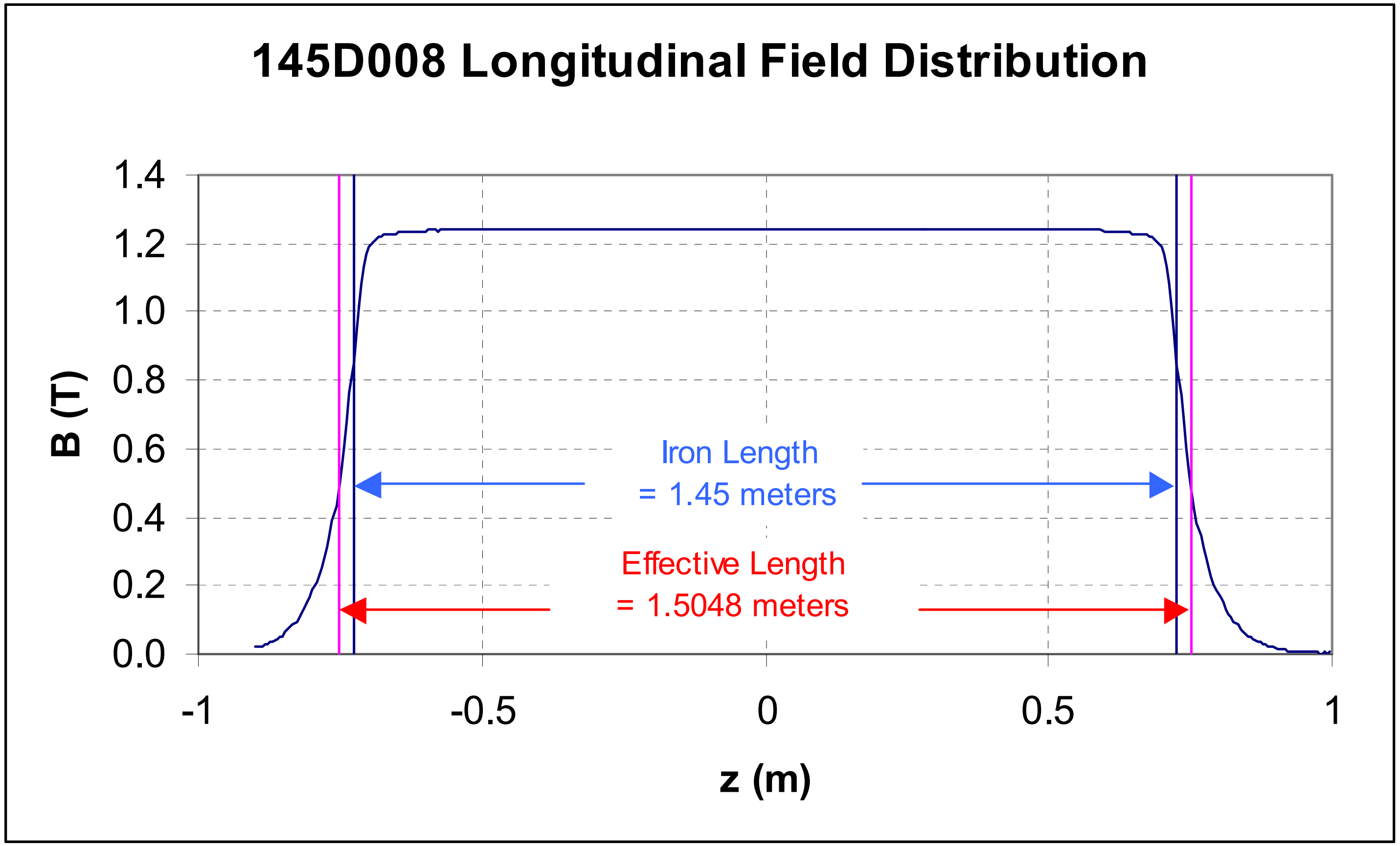

Effective length Dipole magnet $L_{eff}=\int Bds/B_o$

Quadrupole magnet $L_{eff}=\int Gds/G_o$

Sextupole magnet $L_{eff}=\int Sds/S_o$

Magnet end chamber or shim on lattice magnet

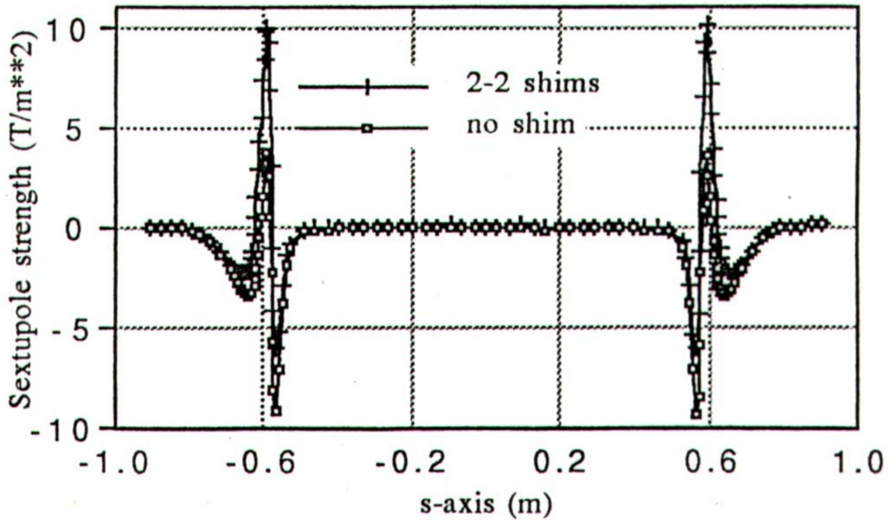

Dipole end shim

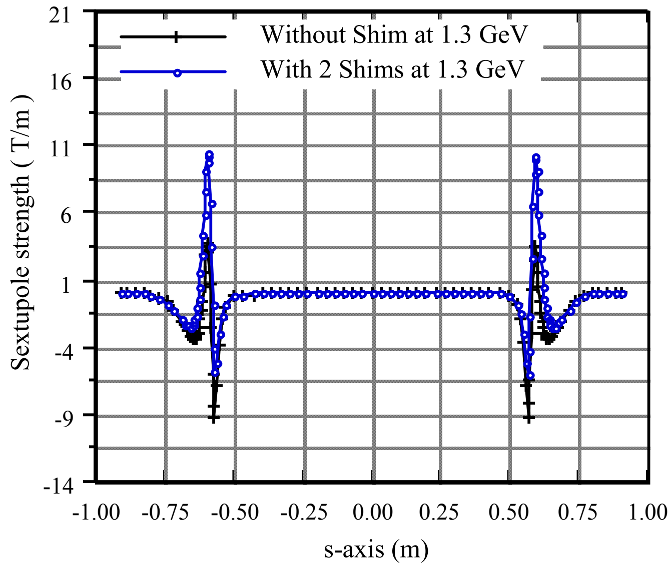

Dipole end shim

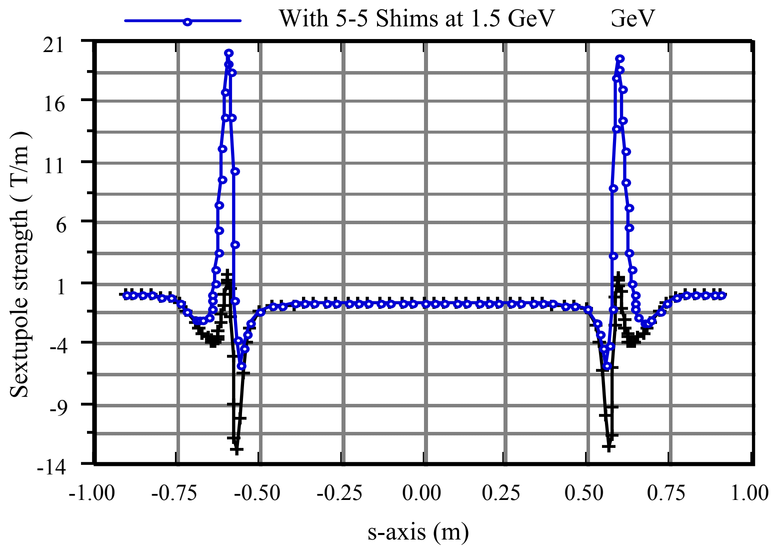

Dipole end shim

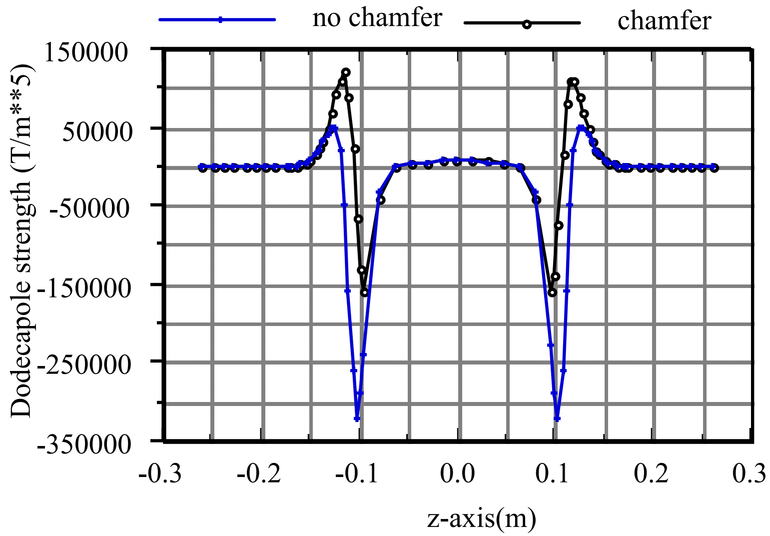

Quadrupole end chamber

Magnet end chamber & shim at the pole end

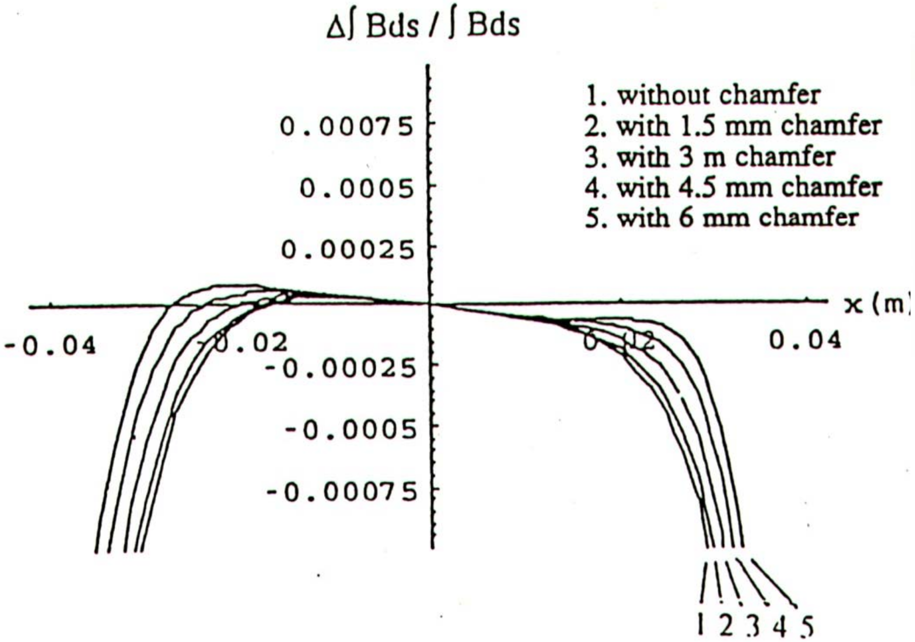

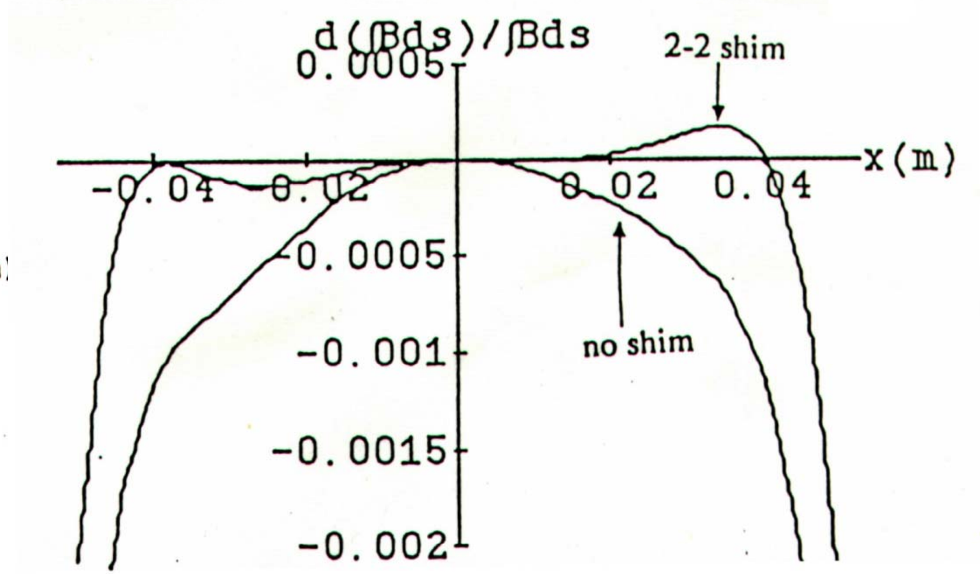

Quadrupole integral field strength distribution w & w/o end chamber

Dipole integral field strength distribution w & w/o end shim

Dipole magnet analysis of the field measurement

Dipole magnet shown in Fig1- 8

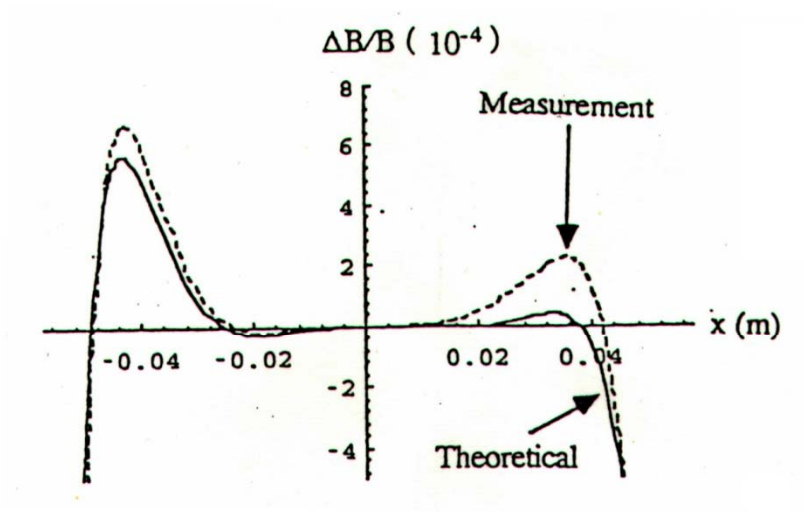

Fig1 The field deviation as a function of x of the two dimensional theoretical calculation, and the measurement results of the combined function bending magnet. Where the field deviation definition is

$$\Delta B / B = \left[B(x) - \left(a_1 + a_2 x\right)\right] / B(x)$$

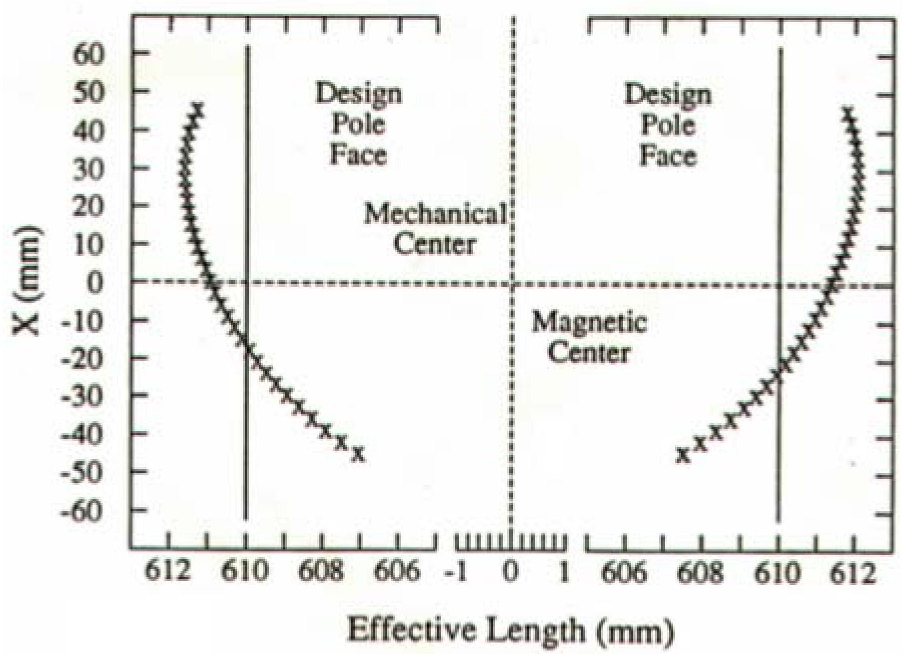

Fig2 NSRRC magnet measure dipole data for magnet field effective length BL/B0

Quadrupole magnet analysis of the field measurement

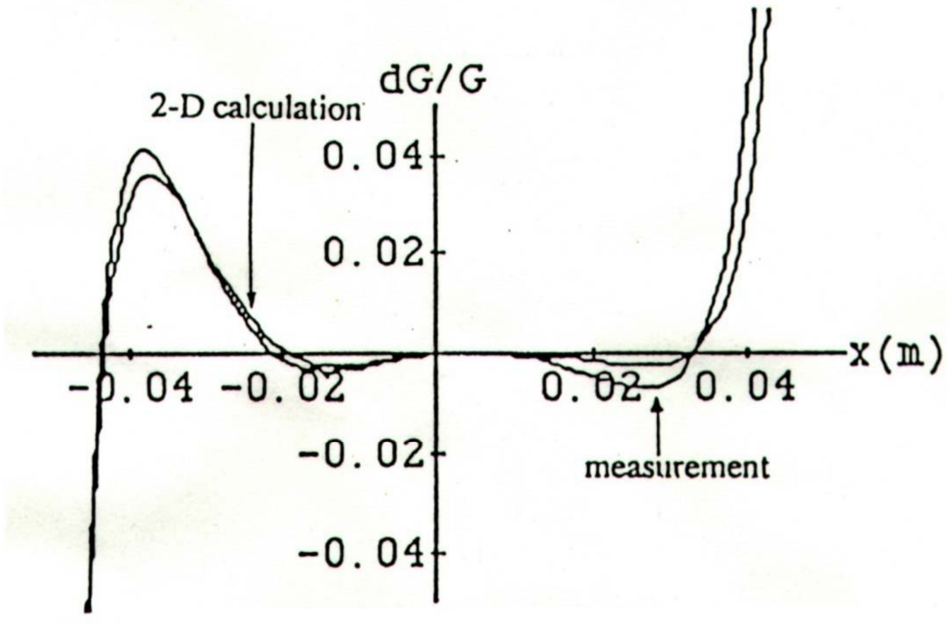

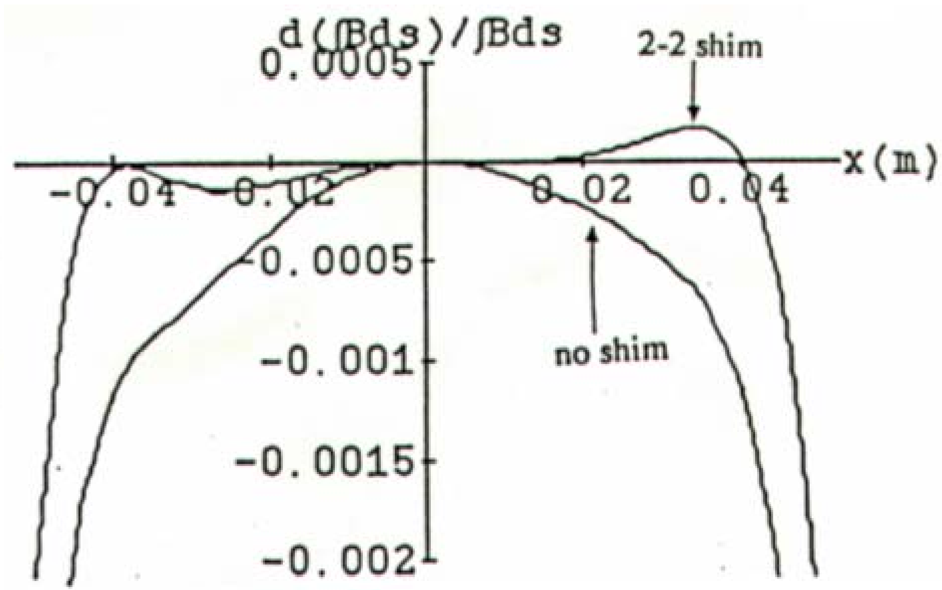

Fig3 The gradient field deviation of the 2-D calculation and measurement results at the magnetic center.

Fig4 After and before 2-2 shims measurement results of the integrated field deviation

The results of field measurement NSRRC dipole magnet

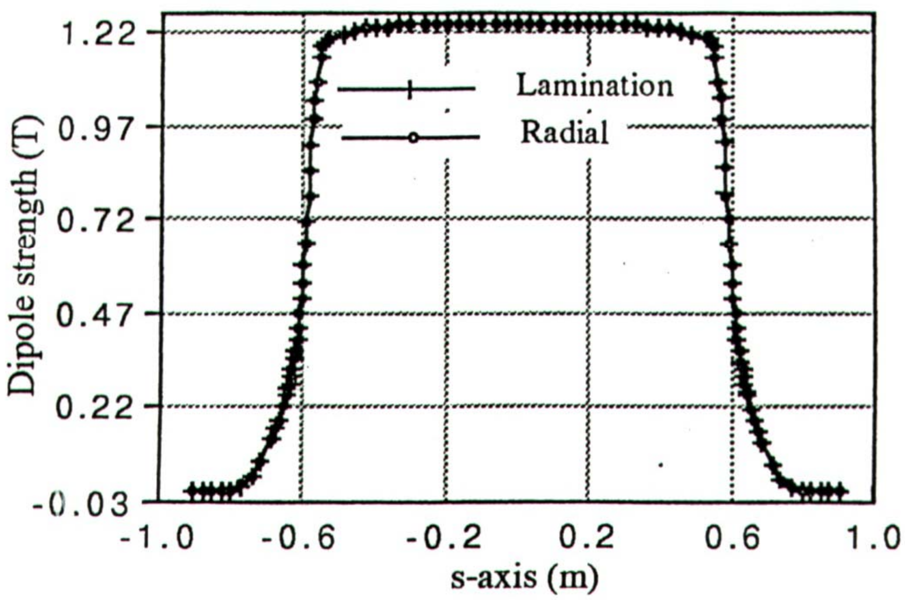

Fig5 The dipole field distribution of the radial and lamination mapping along the beam direction

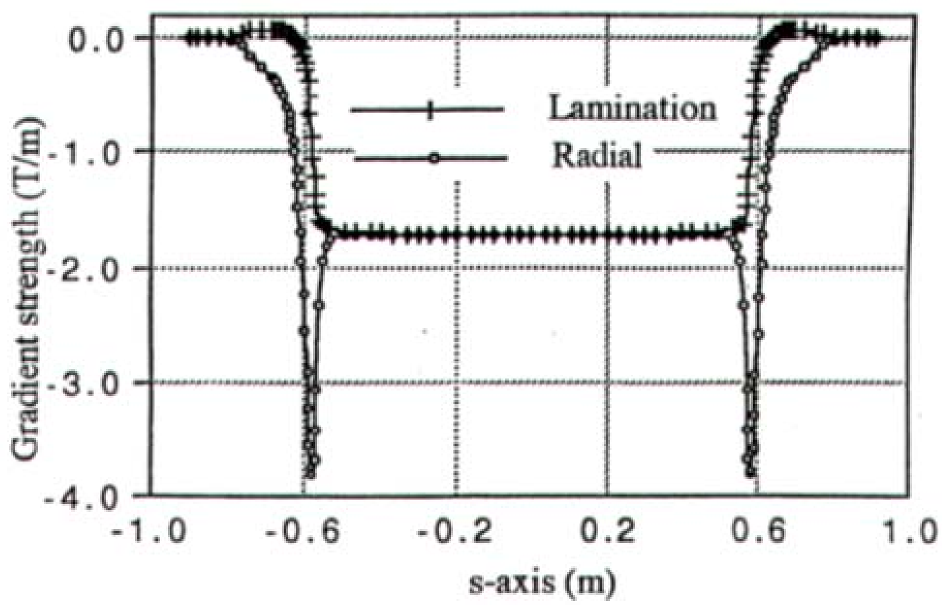

Fig6 The gradient field distribution of radial and lamination mapping along the beam direction

The results of field measurement SRRC dipole magnet

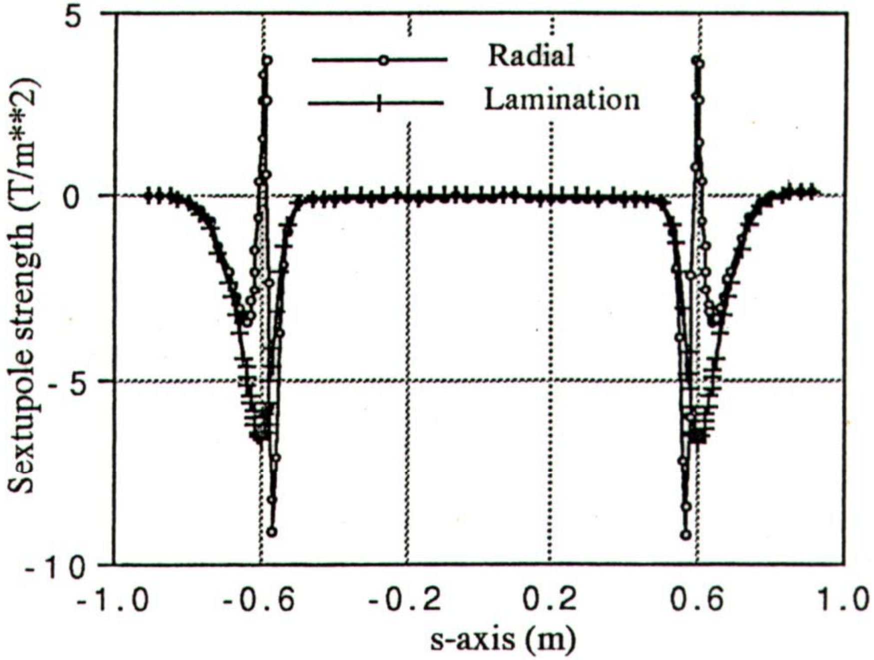

Fig7 The sextupole distribution of the radial and lamination mapping along the beam direction

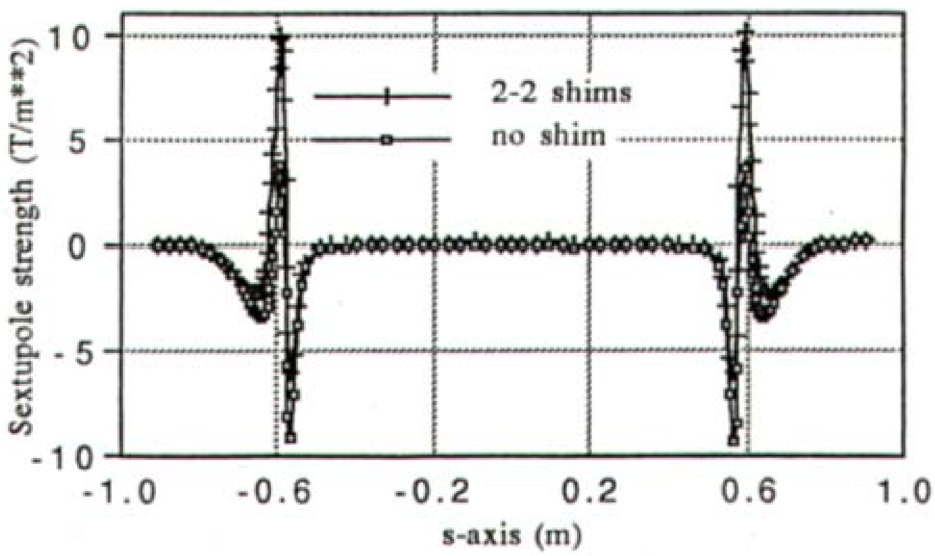

Fig8 The sextupole field distribution along the beam direction of the after and before 2-2 shims measurement results

Dipole end shim

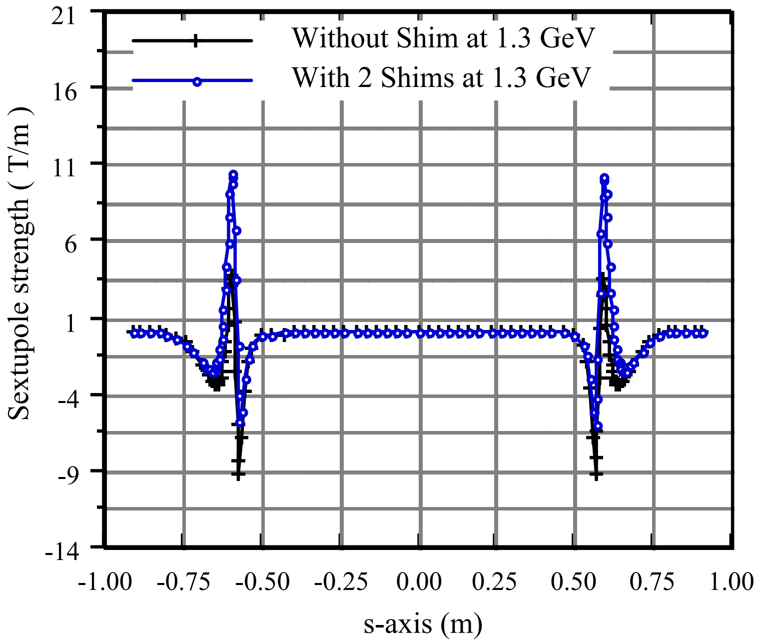

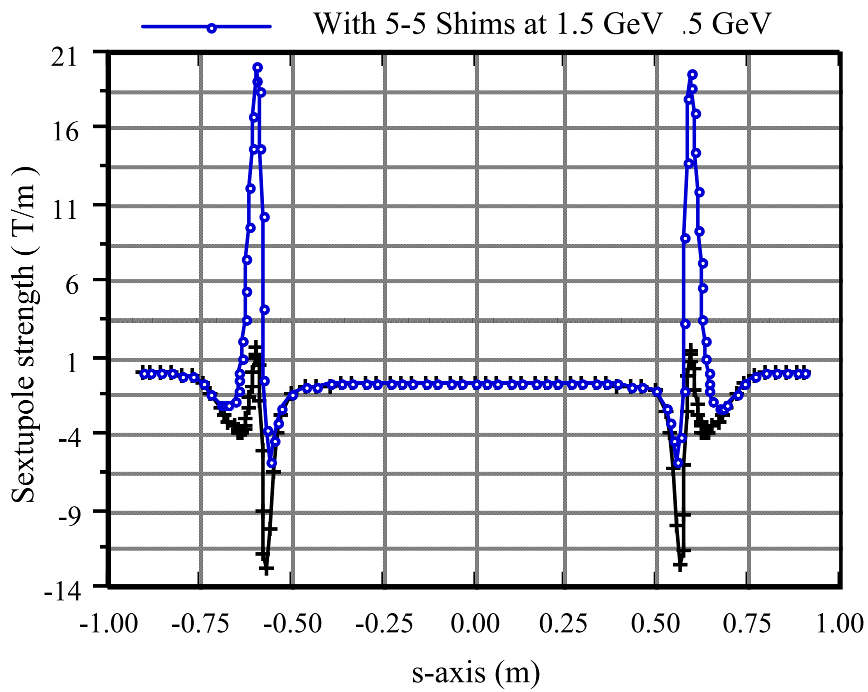

The results of field measurement NSRRC quadrupole magnet

Quadrupole magnet shown in Fig9-10

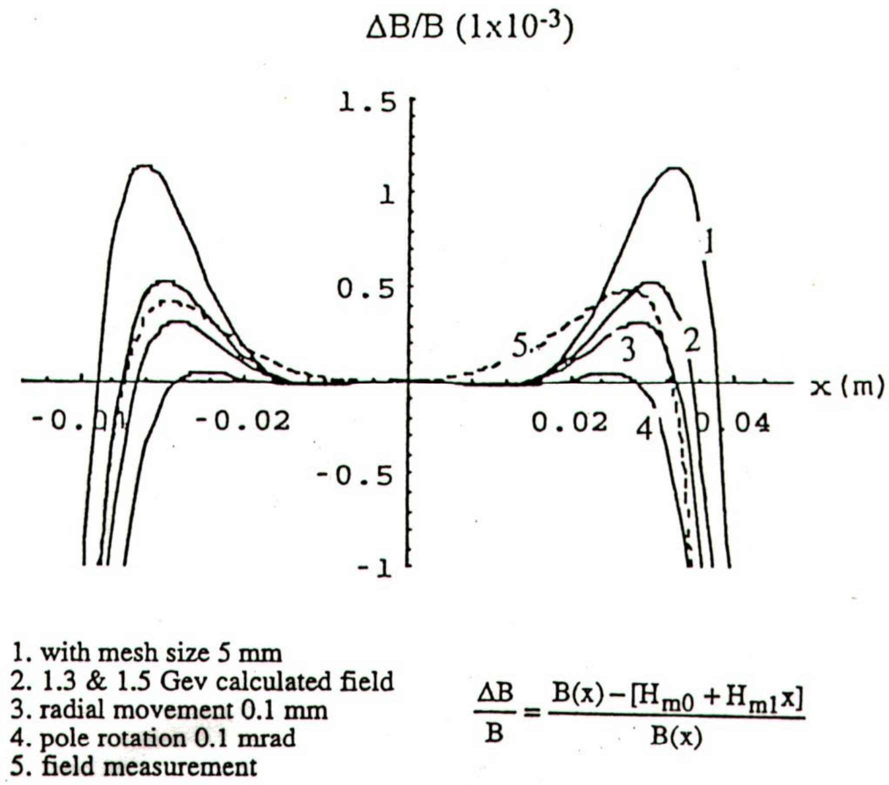

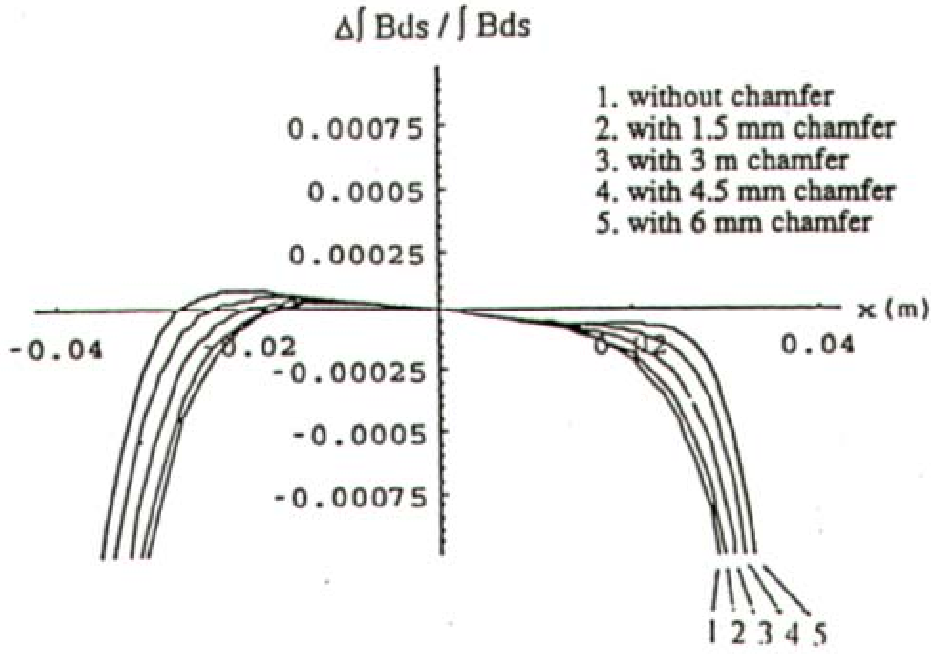

Fig9 The field deviation as a function of transverse direction of the 2-D and measurement results on the midplane

Fig10 The deviation of integrated field with different thickness chamfering